R. & M. No. 2577
(10280, 11610)
A.R.C. Technical Report

MINISTRY OF SUPPLY

AERONAUTICAL RESEARCH COUNCIL
REPORTS AND MEMORANDA

The Theoretical Estimation of Power Requirements for Slot-suction Aerofoils, with Numerical Results for Two Thick Griffith Type Sections

By

J. H. PRESTON, B.Sc., Ph.D., N. GREGORY, B.A., and A. G. RAWCLIFFE, B.A.,
of the Aerodynamics Division, N.P.L.

LONDON: HER MAJESTY'S STATIONERY OFFICE
1953
PRICE 7*s* 6*d* NET

The Theoretical Estimation of Power Requirements for Slot-suction Aerofoils, with Numerical Results for Two Thick Griffith Type Sections

By

J. H. PRESTON, B.Sc., Ph.D., N. GREGORY, B.A., and A. G. RAWCLIFFE, B.A.,
of the Aerodynamics Division, N.P.L.

Reports and Memoranda No. 2577
June, 1948

Summary.—This report describes a method for assessing the performance of slot-suction aerofoils in terms of an effective drag coefficient, which takes into account the power requirements of the suction pump neglecting slot entry and duct losses. When the suction-slot is located at a velocity discontinuity the suction flow required to prevent separation can be calculated, using the elementary theory suggested by Sir Geoffrey Taylor.

The method is applied to two Griffith type aerofoils (30 per cent and 31·5 per cent thick) and the drags are compared with those of normal thin aerofoils 20 per cent thick. When transition is forward the drags are nearly equal; but when transition is at the slot the drags of the suction aerofoils are very much less than that of a normal thin aerofoil with transition at its most rearward feasible position.

The gains afforded by the use of suction near the trailing edge of an aerofoil arise partly from reduction of form drag, and partly from an economy in power when the loss of head in the boundary layer is restored by means of a pump instead of appearing as a loss of momentum in the wake to be overcome by a thrust. Further gains will result if the pump efficiency is greater than the propulsive efficiency.

1. *Notation.*

x	Distance along chord
s	Distance along surface from front stagnation point
c	Chord
y	Distance normal to chord, or when applied to the boundary layer, measured normal to the surface
δ	Boundary-layer thickness
u	Velocity in the boundary layer
U_0	Free-stream velocity
U	Velocity at edge of boundary layer
p	Pressure in the fluid
h	Total head of the fluid

Published with the permission of the Director, National Physical Laboratory.

θ Momentum thickness, $= \int_0^\delta \frac{u}{U}\left(1 - \frac{u}{U}\right) dy$

Suffices 1 and 2 applied to u, U, p and θ refer to conditions immediately upstream and downstream of the discontinuity, respectively.

R Reynolds number

R_θ $\theta U/\nu$

H Boundary-layer shape parameter, = ratio of displacement to momentum thicknesses

$\frac{\tau_0}{\rho U^2}$ A coefficient of local skin friction $\equiv c_f/2 \equiv (u_\tau/U)^2$

λ Pohlhausen boundary-layer parameter $= \frac{\delta^2}{\nu}\frac{dU}{ds}$

Q Rate of boundary-layer suction flow per unit span

C_Q Suction quantity coefficient $= Q/U_0 c$

H_1 Mean loss of head in boundary layer abstracted at the slot entry

H_2 Loss of head in slot entry and ducting to pump

H_3 Loss of head in exit ducting

η_1 Efficiency of propulsive unit

η_2 Efficiency of pump

P_p Power required by pump

P_t Total power required

C_{Di} Induced-drag coefficient

C_{D0} Profile-drag coefficient, $= 2\theta_0/c$ where θ_0 is momentum thickness far downstream

C_{Dp} Equivalent pump drag coefficient

C_{De} Effective drag coefficient of wing $= C_{Di} + C_{D0} + C_{Dp}$.

---

2. *Introduction.*—The present report describes an approximate method of calculating the profile-drag coefficients and the suction quantity and pump power requirements for suction aerofoils from a knowledge of the designed potential-flow velocity distribution over the aerofoil surface. The method is particularly applicable to the type of aerofoil with a velocity discontinuity. The flow conditions in the neighbourhood of the discontinuity are considered in some detail, and a theory suggested by Sir Geoffrey Taylor and given by Richards[1] (1944) is used to give a measure of the amount of suction required for prevention of boundary-layer separation. The premises of this theory have been investigated experimentally by Gregory[2] (1947), and the suction quantities measured in experiments on various suction aerofoils by Richards (1944),[1] (1945)[3] and Gregory[4] (1946) have proved to be in fair agreement with the theory.

To illustrate the method, the drag and suction coefficients of two particular aerofoils (the GLAS II and the 30 per cent symmetrical Griffith section) are estimated, and the results are compared with existing experimental information and with the drag coefficients of normal thin aerofoils.

The method and examples should be of considerable service to designers who contemplate using a Griffith type of section, since present experiments are of necessity limited to Reynolds numbers between 10^6 and 3×10^6. These, whilst checking the broad principles of the method of design, give little indication of the performance at full-scale Reynolds numbers.

3. *Definition of the Power and Quantity Coefficients for a Suction Wing.*

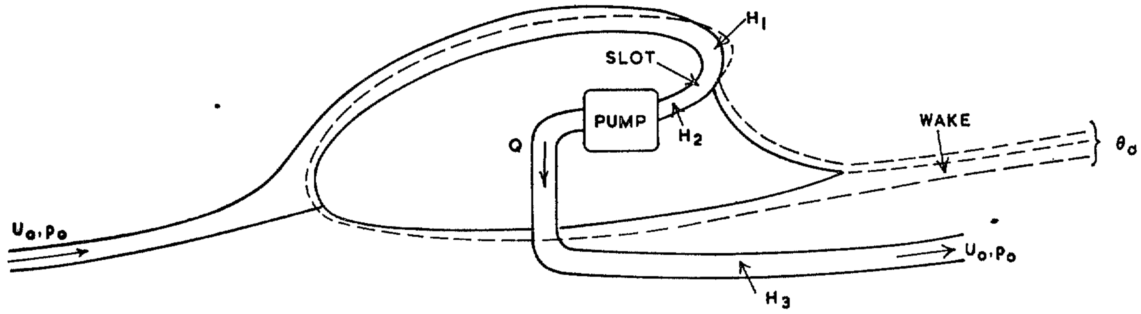

Let the quantity of air sucked at the aerofoil slot in unit time be Q per unit span, with non-dimensional coefficient $C_Q = Q/U_0c$.

Let H_1 be the mean loss of total head in the quantity Q of the boundary layer at the slot entry,
H_2 be the loss of head sustained in the slot entry and ducting to the pump,
H_3 be the loss of head in the exit ducting when the sucked air Q is discharged at free-stream total head,
η_2 be the pump efficiency.

Then the power required by the pump per unit span is

$$P_p = \frac{Q}{\eta_2}(H_1 + H_2 + H_3) \quad \ldots \quad (1)$$

Denote by C_{Di} the induced drag and by C_{D0} the profile drag, which is related to the momentum thickness far downstream, θ_0, by the equation

$$C_{D0} = 2\theta_0/c\ .$$

If η_1 is the efficiency of the propulsion unit which provides the thrust to overcome the induced and profile drags, then the total power required per unit span,

$$P_t = \frac{1}{\eta_1}\left[C_{Di} + C_{D0}\right]\tfrac{1}{2}\rho U_0^3 c + P_p\ ,$$

$$= \frac{1}{\eta}\cdot\tfrac{1}{2}\rho U_0^3 c\left[C_{Di} + C_{D0} + \frac{\eta_1}{\eta_2}\cdot C_Q\cdot\frac{(H_1 + H_2 + H_3)}{\tfrac{1}{2}\rho U_0^2}\right]. \quad \ldots \quad (2)$$

Hence the term $\frac{\eta_1}{\eta_2}\cdot C_Q\cdot\frac{H_1 + H_2 + H_3}{\frac{1}{2}\rho U_0^2}$ can be regarded as the 'equivalent' drag coefficient for the pump. It is a complicated coefficient requiring knowledge of the propulsive efficiency η_1 and the pump efficiency η_2, which are only available in the design stage. In what follows, we take $\eta_1 = \eta_2$; if this does not apply in actual design, then a correction can be made. We also ignore the terms H_2 and H_3, which represent the slot entry and duct losses, and are not known in any particular case until experiments have been made. It is possible that by the use of a wide slot and a duct of large cross-sectional area, H_2 and H_3 can be made small compared with H_1.

Hence we take as the 'ideal' pump-drag coefficient,

$$C_{Dp} = C_Q\cdot\frac{H_1}{\frac{1}{2}\rho U_0^2} = C_Q\cdot\frac{H_1}{\frac{1}{2}\rho U_1^2}\cdot\left(\frac{U_1}{U_0}\right)^2, \quad \ldots \quad (3)$$

where U_1 is the velocity at the edge of the boundary layer just upstream of the slot.

Ignoring the induced-drag coefficient which depends on the wing plan form, we form an 'ideal effective' drag coefficient for suction aerofoils,

$$C_{De} = C_{D0} + C_{Dp}\,, \qquad \qquad (4)$$

which can be compared with the profile-drag coefficients of normal aerofoils.

4. *The Fundamental Economy of Boundary-layer Suction.*—The power required to propel a body of any shape is less if the boundary layer due to the body has its loss of head restored, rather than if it were allowed to appear as a loss of momentum in the wake to be balanced by a thrust created by an increase of momentum elsewhere. For in the latter case power is wasted as kinetic energy, not only in the wake, but also in the slipstream. On the other hand, there is no loss of kinetic energy if the boundary layer at the trailing edge has its total head restored by a pump.

This is true for aerofoils of any thickness or shape, but for simplicity let us consider one side of a flat plate of finite length. Let suffix 0 refer to conditions far upstream and suffix 1 to conditions at the trailing edge.

Outside the boundary layer the total head of the fluid, h, is constant;

$$h_0 = p_0 + \tfrac{1}{2}\rho U_0^2\,.$$

Consider a stream filament in the boundary layer which has total head

$$h_1 = p_0 + \tfrac{1}{2}\rho u_1^2\,.$$

If the boundary layer is sucked at the trailing edge, then the pump power required to restore the total head of the boundary layer is given by

$$\begin{aligned} P_p &= \int_0^\infty (h_0 - h_1)u_1\,dy \\ &= \int_0^\infty \tfrac{1}{2}\rho(U_0^2 - u_1^2)u_1\,dy \\ &= \tfrac{1}{2}\rho U_0^3 \int_0^\infty \frac{u_1}{U_0}\left[1 - \left(\frac{u_1}{U_0}\right)\right]^2 dy\,, \end{aligned}$$

and the pump-drag coefficient is given by

$$\begin{aligned} C_{Dp} &= \frac{1}{c}\int_0^\infty \frac{u_1}{U_0}\left[1 - \left(\frac{u_1}{U_0}\right)^2\right] dy \\ &= \frac{1}{c}\int_0^\infty \frac{u_1}{U_0}\left(1 - \frac{u_1}{U_0}\right)\left(1 + \frac{u_1}{U_0}\right) dy\,. \end{aligned} \qquad \qquad (5)$$

If, however, the boundary layer leaves the trailing edge, forming a wake, the loss of momentum, or drag, is equal to

$$\int_0^\infty \rho u_1\,(U_0 - u_1)\,dy\,.$$

The power required to overcome this is

$$\begin{aligned} P_{\text{thrust}} &= U_0 \int_0^\infty \rho u_1\,(U_0 - u_1)\,dy\,, \\ &= \rho U_0^3 \int_0^\infty \frac{u_1}{U_0}\left(1 - \frac{u_1}{U_0}\right) dy\,, \end{aligned}$$

or the drag coefficient

$$C_{D0} = \frac{2}{c}\int_0^\infty \frac{u_1}{U_0}\left(1 - \frac{u_1}{U_0}\right) dy\,. \qquad \qquad (6)$$

Now comparing (5) and (6) it is seen, since u_1 is by definition less than U_0, that $(1 + u_1/U_0) < 2$, and so $C_{Dp} < C_{D0}$. If the boundary layer consisted entirely of completely stagnant air, C_{Dp} would then be exactly one half of C_{D0}. These results appear to have been known to Ackeret[15] (1938), though they were derived independently by us in the course of this work.

The variation of the ideal effective drag coefficient of a flat plate with the amount of boundary layer sucked is shown for laminar and turbulent boundary-layer profiles in Fig. 1. It is seen that by sucking the whole boundary layer when the flow is laminar, C_{De} is 79 per cent of C_{D0} without suction. For turbulent flow the ratio is less, depending on Reynolds number, a rough figure being 92 per cent.

This result only holds if the slot is at the extreme rear of the plate. If the slot is forward of the trailing edge, a fresh boundary layer starts behind the slot, and the local intensity of skin friction there is high. The variation of ideal effective drag coefficient with slot position is shown for a flat plate in Fig. 2.* It is seen that there is a saving of drag only if the slot is to the rear of 0·94 chord for laminar flow, or 0·90 chord for turbulent flow. If the slot is well forward, there can be about 25 per cent increase in drag for a laminar boundary layer. The addition of a second slot located at the trailing edge reduces the drag for all positions of the first slot, and slightly extends the range of front slot position over which the arrangement is more economical than the plate without any slots.

Thus the potential economy of boundary-layer suction can only be realised on a flat plate if the slot is very close to the trailing edge. This result also holds for a shaped body. But in both cases boundary-layer suction at a slot or slots other than at the trailing edge may be attractive for other reasons, for example:—

(1) Separation of the boundary layer may be prevented, thus enabling high $C_{L\,max}$ to be obtained, or as suggested by Goldstein and Richards, allowing aerofoils of exceptional thickness to be utilised so that all wing aircraft can be designed at a much smaller all-up weight than was formerly possible.

(2) Regions of turbulent flow may be replaced by regions of laminar flow.

(3) The pumping system may be more efficient than the propulsive system. In the case of jet-propelled aircraft, the system is comparable with propeller turbine installations and enables aircraft using gas turbines to be flown at relatively low cruising speeds with good efficiency.

5. *Behaviour of the Boundary Layer at a Discontinuity.—Taylor's Theory.*—This section considers the behaviour of the boundary layer at the position of velocity discontinuity on a Griffith type suction aerofoil.

It is obvious that if the suction slot were located just ahead of the discontinuity, and that if all the boundary layer were sucked away, then the flow would cross the discontinuity without separation occurring, as potential flow would exist at this point.

On the other hand, if all the boundary layer is not sucked away, there must be a considerable thickening and possible separation of the remainder as it passes through the short region of severe adverse gradient, or theoretical discontinuity.

The theory suggested by Sir Geoffrey Taylor gives us a means of estimating the minimum quantity which will have to be sucked to prevent separation of the boundary layer.

The following assumptions are made,

(a) that the pressure is constant across the boundary layer,

(b) that the total head is constant along streamlines in the boundary layer as they cross the discontinuity.

* For the calculation of this figure, the momentum thickness was assumed to be proportional to $x^{1/2}$ and $x^{4/5}$ for laminar and turbulent flow respectively.

The truth of (b) has been experimentally confirmed by Gregory[2] (1947). The first assumption, (a), is not accurate, but R. & M. 2496[2] has shown that the effects of pressure variation are roughly balanced by the resultant changes in velocity at the edge of the boundary layer, and hence in effective velocity discontinuity. The form of the theory given below, which neglects curvature of the surface, still gives a good approximation to suction quantity.

If subscripts 1 and 2 refer to positions just upstream and downstream of the discontinuity, then at the edge of the boundary layer

$$p_1 + \tfrac{1}{2}\rho U_1^2 = p_2 + \tfrac{1}{2}\rho U_2^2 ,$$

and in the boundary layer

$$p_1 + \tfrac{1}{2}\rho u_1^2 = p_2 + \tfrac{1}{2}\rho u_2^2 .$$

Hence

$$u_2^2 = u_1^2 - (U_2^1 - U_2^2) , \quad \ldots \quad (7)$$

$$\text{or } \frac{u_2}{U_2} = \sqrt{1 - \left(\frac{U_1}{U_2}\right)^2 \left[1 - \left(\frac{u_1}{U_1}\right)^2\right]} . \quad \ldots \quad (8)$$

Now for u_2 to be real,

$$u_1^2 \geqslant U_1^2 - U_2^2 \quad \text{or} \quad \left(\frac{u_1}{U_1}\right)^2 \geqslant 1 - \left(\frac{U_2}{U_1}\right)^2 \quad \ldots \quad (9)$$

For a given aerofoil U_2/U_1 is known, and hence for any boundary-layer velocity profile in front of the discontinuity the fluid between the wall and the filament where $u_1/U_1 = \sqrt{\{1-(U_2/U_1)^2\}}$ must be sucked away for real values of u_2/U_2 to exist downstream of the discontinuity.

This argument gives us a minimum quantity to be sucked in order to prevent separation. The effect of sucking greater quantities is discussed later (*see* sections 6.2 and 7.5), but we shall here continue the argument assuming for the moment that the minimum quantity is sucked.

Let $(y_1)_0$ be the distance from the surface of the filament specified by $(u_1/U_1)_0 = \sqrt{\{1-(U_2/U_1)^2\}}$. Then the suction quantity for unit span is given by

$$Q = \int_0^{(y_1)_0} u_1 \, dy_1, \text{ or } \frac{Q}{U_1\theta_1} = \int_0^{y_1 = (y_1)_0} \frac{u_1}{U_1} \, d\left(\frac{y_1}{\theta_1}\right) , \quad \ldots \quad (10)$$

and may be expressed in coefficient form as

$$C_Q = \frac{Q}{U_0 c} = \frac{Q}{U_1\theta_1} \cdot \frac{U_1}{U_0} \cdot \frac{\theta_1}{c} . \quad \ldots \quad (11)$$

For a filament which is not removed through the slot, continuity gives

$$u_1 \, dy_1 = u_2 \, dy_2 . \quad \ldots \quad (12)$$

Hence

$$y_2 = \int_{(y_1)_0}^{y_1} \frac{u_1}{u_2} \, dy_1 . \quad \ldots \quad (13)$$

Equations (8) and (13) enable us to construct the downstream profile*.

The change in boundary-layer momentum thickness can be found from the relation

$$\frac{\theta_2}{\theta_1} = \int_0^\infty \frac{u_2}{U_2}\left(1 - \frac{u_2}{U_2}\right) d\left(\frac{y_2}{\theta_1}\right) ,$$

but from (12)

$$u_1 d\left(\frac{y_1}{\theta_1}\right) = u_2 d\left(\frac{y_2}{\theta_1}\right) .$$

* There is a singularity in the integrand of (13) when $u_1 = (u_1)_0$ since this makes $u_2 = 0$. The integration can be started by expressing u_1 as a Taylor series in the neighbourhood of $u_1 = (u_1)_0$.

Therefore $$\frac{\theta_2}{\theta_1} = \int_{y_1=(y_1)_0}^{\infty} \left(\frac{u_1}{U_1}\right)\left(\frac{U_1}{U_2}\right)\left(1-\frac{u_2}{U_2}\right) d\left(\frac{y_1}{\theta_1}\right), \quad \ldots \quad (14)$$

where u_2/U_2 is given by equation (8).

The loss of head of the boundary-layer filament with velocity u_1 is $\frac{1}{2}\rho(U_1^2 - u_1^2)$. Hence the mean loss of head H_1, in the sucked portion Q, is found to be given by

$$\frac{H_1}{\frac{1}{2}\rho U_1^2} = \frac{\int_0^{y_1=(y_1)_0} \frac{u_1}{U_1}\left[1-\left(\frac{u_1}{U_1}\right)^2\right] d\left(\frac{y_1}{\theta_1}\right)}{\int_0^{y_1=(y_1)_0} \frac{u_1}{U_1}\, d\left(\frac{y_1}{\theta_1}\right)}. \quad \ldots \quad (15)$$

Whence, from equation (3), the ideal pump-drag coefficient is given by

$$C_{Dp} = \frac{\theta_1}{c}\left(\frac{U_1}{U_0}\right)^3 \int_0^{y_1=(y_1)_0} \frac{u_1}{U_1}\left[1-\left(\frac{u_1}{U_1}\right)^2\right] d\left(\frac{y_1}{\theta_1}\right), \quad \ldots \quad (16)$$

a relation similar to that obtained in equation (5) for a flat plate.

6. *The Method of Estimation of Quantity and Drag Coefficients.*—In this section, the growth of the boundary layer is traced progressively from the front stagnation point to the trailing edge of the aerofoil. The behaviour of the boundary layer at the discontinuity is quickly found in any particular case from graphs compiled on the analysis of the previous section.

6.1. *Calculation of the Boundary Layer from Leading Edge to the Slot.*—The value of the momentum thickness just in front of the slot can rapidly be calculated from several different formulae, each representing an approximate integration of the momentum equation.

(a) For the laminar layer, the momentum thickness θ can be obtained by the simplified method of Falkner[5] (1941), who shows that an approximate universal relation exists between $(\theta/s)(Us/\nu)^{1/2}$ and an integral

$$I_3 = \frac{1}{U^6 s}\int U^6\, ds. \quad \ldots \quad (17)$$

The momentum thickness can also be computed using the general method given by Tetervin[6] which is similar to that proposed earlier by Holt[7] (1943). If H, the boundary-layer shape parameter, is assumed constant, and a relation between $\tau_0/\rho U^2$ and R_θ ($=U\theta/\nu$) of the type

$$\frac{\tau_0}{\rho U^2} = \frac{k}{R_\theta^{\,m}} \quad \ldots \quad (18)$$

is assumed, then the momentum equation can be integrated and θ can be found. The relation is

$$\left[\left(\frac{\theta}{c}\right)^{m+1}\left(\frac{U}{U_0}\right)^{\overline{H+2}.\overline{m+1}}\right]_A^B = \frac{(m+1)k}{R_c^{\,m}}\int_A^B \left(\frac{U}{U_0}\right)^{\overline{H+1}.\overline{m+1}+1} d\left(\frac{s}{c}\right). \quad \ldots \quad (19)$$

For laminar flow we take the Blasius skin-friction law and boundary-layer velocity profile, giving $m=1$, $k=0\cdot2205$ and $H=2\cdot591$.

Another solution for the general laminar boundary layer is that proposed by Thwaites[8] (1947),

$$\left(\frac{\theta}{c}\right)^2 = \frac{0\cdot45}{R_c(U/U_0)^6}\int\left(\frac{U}{U_0}\right)^5 d\left(\frac{s}{c}\right). \quad \ldots \quad (20)$$

All these approximations are reasonably accurate in regions of increasing velocity where laminar flow is likely to occur. At the transition position we assume the momentum thickness to be continuous, and use the value given by the laminar-flow relation to be the initial value in the turbulent region.

(b) In the turbulent region we use the Tetervin relation, equation (19). The constants m and k can be chosen to give a wide range of agreement with the pipe flow relation in the manner suggested by Tetervin. The relation chosen for the examples in this paper was

$$\frac{\tau_0}{\rho U^2} = \frac{0\cdot00976}{R_\theta^{\,0.2075}}, \qquad \qquad (21)$$

which is shown plotted in Fig. 3 for comparison with the existing and more complicated relations.* In the region of favourable or only slightly adverse gradient, H should be taken as $1\cdot4$, but when the adverse gradient is large (as on the lower surface of GLAS II toward the tail), it would be better to use a value of $1\cdot6$. It has been shown by Squire and Young[10] (1937) that the drag is not particularly sensitive to choice of H.

We now consider the boundary-layer velocity profiles.

(a) For laminar flow the velocity profile just ahead of the slot is determined by the local velocity gradient. The profile does not change with Reynolds number although the boundary-layer thickness varies as $R^{-1/2}$. The approximate profile shape can be determined if the profile is assumed to be of the Pohlhausen polynomial type defined by the parameter $\lambda = (\delta^2/\nu)\, dU/ds$ (*see* Ref. 9). The extreme limits of the Pohlhausen profile are illustrated in Fig. 4, together with the profile $\lambda = 0$ which is appropriate to the flow along a flat plate with zero pressure gradient, and this case is found to agree very closely with the exact Blasius flat-plate profile.

However, owing to the uncertainty in the velocity gradient just in front of the slot, due to the sink effect varying with different suction quantities, the actual velocity profile† cannot be found, except possibly with great labour for the laminar case. Therefore, the flat-plate profile $\lambda = 0$ as a mean, is used for the calculations.

(b) When the flow is turbulent in front of the slot, there is no satisfactory method of estimating the velocity distribution through the boundary layer under pressure gradients. If these are small, however, it may be assumed that the profile is not greatly different from the pipe-flow distribution, namely

$$\left.\begin{aligned} &\frac{u}{U} = 1 + \frac{1}{K}\cdot\frac{U_\tau}{U}\log_e(y/\delta)\,, \\ \text{where}\quad &K = 0\cdot4\,, \\ \text{and}\quad &\frac{U_\tau}{U} = \left(\frac{c_f}{2}\right)^{1/2} = \left(\frac{\tau_0}{\rho U^2}\right)^{1/2}. \end{aligned}\right\} \qquad (22)$$

This distribution was used by von Kármán in the case of the flat plate under zero pressure gradient. It is found that

$$\frac{\theta}{\delta} = \frac{U_\tau}{KU} - 2\left(\frac{U_\tau}{KU}\right)^2, \qquad \qquad (23)$$

so that the velocity profile is a function of $\tau_0/\rho U^2$. It is assumed that $\tau_0/\rho U^2$ is a function of $R_\theta (= U\theta/\nu)$ only, and that the relation found for turbulent flow (equation (21)) can be taken to apply. Thus when θ is found, the velocity profile is fixed.

The turbulent velocity profiles are plotted in Fig. 4 for values of $\tau_0/\rho U^2$ corresponding approximately to Reynolds numbers $(= Ux/\nu)$ of 10^6, 10^7, and 10^8.

In evaluating equation (14) it was more convenient to use the algebraic 'power' law $u/U = (y/\delta)^{1/n}$. These profiles approximate closely to the logarithmic profiles at Reynolds numbers of 10^6, 10^7 and 10^8 if the index n is taken successively as 9, 11 and 13.

---

* It is seen that considerable differences exist in the various formulae which have been proposed, due to the seeking of an explicit relation which would give a good fit to the rather scattered experimental results. In view of its importance in drag calculation, it would seem worthwhile to repeat the experiments over a wide range of Reynolds number.

† In addition the distortion of the field, due to curvature of the surface, is neglected in this paper.

6.2. *Crossing the Discontinuity.*—We start with a knowledge of the value of the velocity discontinuity, the state of the flow (laminar or turbulent), and the momentum thickness θ_1/c at the slot.

Fig. 5, which was obtained from equation (10), gives $Q/U_1\theta_1$, as a function of U_2/U_1, where Q is the minimum suction quantity given by Taylor's theory, and it enables the suction quantity coefficient to be written down from equation (11).

The mean loss of head of the sucked boundary layer $H_1/\frac{1}{2}\rho U_1^2$ obtained from equation (15) is given in Figs. 6a and b as functions of the suction quantity and of the velocity discontinuity.

The ideal pump-drag coefficient, equation (3), can be found directly from the graph of Fig. 7. This figure was compiled from equation (16).

In Figs. 5, 6b and 7 where the abscissa is U_2/U_1, the value of the discontinuity when suction is according to Taylor's criterion, U_2/U_1 can be replaced by $\sqrt{\{1 - (u_1/U_1)^2\}}$ where u_1/U_1 is the value of the outermost filament that is sucked. This enables the graphs to be used when the suction quantity is greater than that given by Taylor's criterion, or when the criterion does not apply because of the absence of a discontinuity. Thus, the mean loss of total head and the pump-drag coefficient can be found from a fictitious U_2/U_1 corresponding to the discontinuity for which the specified suction quantity would be a minimum.

The change in momentum thickness across the slot is given in Fig. 8, where θ_2/θ_1 is plotted as a function of U_2/U_1 (from equation (14)), for suction according to Taylor's criterion only. For other suction quantities Fig. 9 must be used, which shows, for laminar profile and for turbulent profiles at a Reynolds number of 10^7, θ_2/θ_1 as a function of $Q/U_1\theta_1$ for several values of the discontinuity.

In illustration of the theory, some velocity profiles downstream of a discontinuity derived from standard profiles upstream of the discontinuity by means of equations (8) and (13) are shown in Fig. 10. When the upstream flow is laminar the downstream profile is very similar to the initial one, with slight thickening. When the flow is turbulent the downstream profiles are markedly different and the boundary-layer thickness is much greater. However, as shown in Fig. 10b, with a slight increase in suction the boundary-layer thickness and the momentum thickness downstream are very much reduced. This is in agreement with Fig. 9.

6.3. *Growth of the Boundary Layer Downstream of the Slot to the Trailing Edge.*—This calculation follows the same lines as that of section 6.1. The flow should be taken as turbulent if the surface behind the slot is concave. The initial value of the momentum thickness will be θ_2 as given above. From the final value of the momentum thickness at the trailing edge $\theta_{\text{T.E.}}$, which should include contributions from both upper and lower surfaces, we obtain the profile-drag coefficient of the aerofoil by the method of Squire and Young[10] (1937).

$$C_{D0} = 2(\theta/c)_{\text{T.E.}}\,(U/U_0)_{\text{T.E.}}^{(H+5)/2}. \qquad (24)$$

H is usually taken as $1\cdot4$ in this formula.

7. *Applications.*—The method of this report is here applied to calculate the power requirements for two thick suction aerofoils, the symmetrical 30 per cent thick Griffith section, and the single-slot cambered aerofoil GLAS II. The calculated results are compared with experimental evidence and with theoretical drag coefficients for normal sections.

The variation of ideal effective drag coefficient with variations of suction quantity from Taylor's minimum quantity up to that of the whole boundary layer is also investigated.

7.1. *Glas II $31\frac{1}{2}$ per cent Single-slot Aerofoil.*—This aerofoil was designed by Glauert[11] (1945) by the exact theory developed by Lighthill[12] (1945). It has only one suction slot (on the upper surface) at which there is a large discontinuity. The aerofoil has $C_{m0} = 0$ and a C_L-range of $0 < C_L < 2\cdot004$. It is shown in Fig. 11 together with the velocity distributions at the limits of the C_L-range.

The growth of momentum thickness* along the surfaces of the aerofoil is shown in Figs. 12 to 15 for the two C_L's, 0 and 2·004 at a Reynolds number of 10^6. Fig. 16a shows the ideal effective drag coefficient C_{D_e} as a function of Reynolds number for various transition positions. It is interesting to note that when $C_L = 2{\cdot}004$ and transition occurs between 0·4 chord and the slot, the drag is closely equal to that when $C_L = 0$. Thus at $C_L = 2{\cdot}004$, the L/D ratio is extremely high.

Figs. 16 b, c and d show the various contributions to C_{D_e} as functions of transition position x/c at Reynolds numbers of 10^6, 10^7 and 10^8 where it is seen that, as transition approaches the slot position, C_{D_e} drops very rapidly. Note the small contribution of the upper surface to the profile, or wake, drag.

The variation of the suction-quantity coefficient with Reynolds number is shown in Fig. 17. At large Reynolds numbers and with laminar flow to the slot, C_Q is very small, and in fact varies as $1/R^{1/2}$. C_Q increases rapidly as the transition position moves forward. For $C_L = 2{\cdot}004$ with transition well forward the C_Q's are roughly double those for $C_L = 0$, when the very favourable pressure gradients result in a thin boundary layer.

7.2. *30 per cent Symmetrical Aerofoil.*—This aerofoil was designed by Richards[3] (1945) on the basis of Goldstein's approximate theory[13] (1942), and is shown with its velocity distribution in Figs. 18a and b. The C_L-range extends from —0·6 to + 0·6.

The growth of momentum thickness along the surface of the aerofoil is shown in Fig. 19 for a C_L of 0 at a Reynolds number of 10^6. The profile-drag coefficients and the ideal effective-drag coefficients are shown in Fig. 20 as functions of transition position for Reynolds numbers of 10^6, 10^7 and 10^8. The variation of C_{D_e} with Reynolds number is given in Fig. 21 where the symmetrical aerofoil is compared with the single-slot aerofoil, GLAS II. It will be noticed that for similar positions of transition the symmetrical aerofoil has a somewhat lower drag than the GLAS II aerofoil.

The variation of suction-quantity coefficient with Reynolds number when $C_L = 0$ is shown in Fig. 22 where it is compared with that for the single-slot GLAS II aerofoil. The latter requires less suction quantity than the twin-slot arrangement, though it should be noted that the slot is at 0·691 chord compared with the 0·8 chord positions for the twin-slot symmetrical section.

7.3. *Comparison of 30 per cent Symmetrical Section Results with Experiment.*—A comparison between theory and experiment is given in Fig. 23a and b for the 30 per cent symmetrical aerofoil. Fig. 23a shows C_Q as a function of transition position at two Reynolds numbers. The trend is for theory to overestimate C_Q, especially when transition is well forward. At the low Reynolds number of $0{\cdot}96 \times 10^6$ with far back transition, the experimental suction quantities were large. This was due to the presence of a troublesome laminar separation caused by the adverse gradient just in front of the slot. As at high Reynolds numbers the closeness of separation (or transition) to the slot raises some doubts as to the velocity distribution in the boundary layer that should be taken as a basis for the calculations.

Fig 23b shows the profile-drag coefficient C_{D_0} as a function of transition position. The theory also tends to overestimate the drag, though the low experimental values of the drag obtained when transition was far back might be accounted for by a short region of laminar flow on the flap which was assumed in the calculation to be turbulent. The disagreements between theory and experiment are commented on further in section 8.

7.4. *Comparison of the Calculated Ideal Effective-drag Coefficients with the Drag Coefficients of Normal Thin Aerofoils.*—The drag coefficients of two low-drag type aerofoils (cusped tails) with maximum velocity at 0·5 chord have been abstracted from the calculations of Lock[14] (1946), and are compared with the C_{D_e} of the two thick aerofoils in the following table.

* The curves of growth of momentum thickness along the surface were obtained for various transition points measured in terms of s/c (the distance along the surface from the front stagnation point). The rest of the results have been cross-plotted and are displayed for various transition points expressed in terms of x/c (the distance along the chord).

Position of Transition Point x/c	Profile-drag Coefficient of Normal Low-drag Aerofoils		Ideal Effective Drag Coefficient		Reynolds Number
	$t/c = 10\%$	$t/c = 20\%$	30% Griffith slots at 0·80 x/c	Glas II slot at 0·691 x/c	
0	0·0122	0·0157	0·0161	0·0192	
0·2	0·0108	0·0138	0·0152	0·0174	
0·4	0·0092	0·0111	0·0130	0·0144	10^6
0·6	0·0068	0·0076	0·0104	0·0100	
slots	—	—	0·0043	0·0067	
0	0·0082	0·0104	0·0112	0·0130	
0·2	0·0069	0·0088	0·0102	0·0113	
0·4	0·0055	0·0067	0·0083	0·0089	10^7
0·6	0·0037	0·0040	0·0058	0·0055	
slots	—	—	0·0016	0·0029	
0	0·0057	0·0072	0·0077	0·0088	
0·2	0·0048	0·0061	0·0069	0·0075	
0·4	0·0036	0·0044	0·0055	0·0058	10^8
0·6	0·0023	0·0024	0·0037	0·0033	
slots	—	—	0·0007	0·0015	

It is seen that when transition is far forward the ideal effective-drag coefficients of both suction aerofoils are slightly greater than those of the 20 per cent thick low-drag section. But when transition is at or just forward of the slots, the drag coefficients of both aerofoils are appreciably lower than the lowest possible drag coefficient for the normal 20 per cent thick aerofoil. The furthest back position of transition for the normal sections has been taken at 0·6 chord. A more rearward transition is unlikely without a subsequent turbulent boundary-layer separation. The suction aerofoils, on the other hand, can be designed to have their slots at 0·8 chord or even nearer the trailing edge.

The drag of the twin-slot aerofoil is less than that of the single-slot aerofoil, for transition forward of mid-chord.

7.5. *Effect of Variation of Suction Quantity on a Thick Suction Aerofoil.*—Following the general analysis of section 6, the variation of ideal effective-drag coefficient with $Q/U_1\theta_1$ for a typical Griffith aerofoil has been worked out for various transition positions and is shown in Figs. 24 and 25. The aerofoil was assumed to have constant velocity gradients as shown in Fig. 24, and to have a slot at 0·80 chord with a moderate velocity discontinuity (2·25:1).

The argument of section 4, illustrated in Fig. 2, shows that an increase in drag occurs when a slot is inserted in a flat plate at the 0·80 chord position and the boundary layer is sucked. On the Griffith type suction aerofoil we find that with a laminar boundary layer the ideal effective-drag coefficient rises as the suction quantity increases from the Taylor quantity to that of the whole boundary layer. On the other hand, if the boundary layer in front of the slot is turbulent there is at first a decrease in C_{De} as the amount of suction is increased. In no case does the variation of ideal effective-drag coefficient exceed 10 per cent whilst the value of $Q/U_1\theta_1$ changes between the minimum Taylor quantity and suction of the whole boundary layer.

8. *Discussion.*—One of the purposes of this report is to give designers and others a method of estimating the drag of Griffith sections. The ideal drag coefficient, as defined, is a figure of merit for comparison with ordinary aerofoils on a strictly aerodynamic basis neglecting entry and duct losses. The extra weight of ducting and pump adds to the drag in an actual design, but on the other hand the greater aerofoil thickness may lead to a lighter structure, and the increased volume of the wing should provide internal stowage space resulting in drag reduction. The overall

advantage of using such wings can only be assessed by design studies, and this report enables the basic aerodynamic data to be obtained quickly by a designer.

In order to obtain an estimate of the ideal drag coefficient a simplified and idealised view of conditions near the slot has been taken. The picture is an over-simplified one for the following reasons:—

(1) Curvature of the flow, and the pressure changes through the boundary layer, are not negligible.

(2) No real discontinuity actually exists, because except at the surface of the aerofoil, the pressure in the boundary layer rises gradually along the streamlines as they cross the 'discontinuity'.

(3) Sink effect on the velocity profiles is not taken into account.

All these influences are neglected, and for routine calculations it would not be practicable to include them, even if the theory could be elaborated to do so. A rigorous attack on the flow conditions in the neighbourhood of the slot, for one case only, would be a very laborious task, and has not yet been successfully attempted.

It is shown in Fig. 23 that for the 30 per cent Griffith aerofoil, when transition is forward, the theoretical profile-drag coefficients are 50 per cent greater than the experimental. The great differences between the actual and the assumed conditions near the slot account for this large discrepancy.

The experimental boundary-layer traverses obtained by Gregory[2] confirm that the minimum suction quantity is that limited by the boundary-layer filament whose total head is equal to the surface static pressure downstream of the slot, and that the total head of filaments crossing the discontinuity is conserved. The report also demonstrates the magnitude of the pressure changes normal to the surface, and the consequent differences in velocity at the edge of the boundary layer from the theoretical values, upstream and downstream of the slot. The ratio of these velocities is much reduced. Thus although confirming the method of estimation of suction quantities, the paper sheds no light on the disagreement between the theoretical and experimental drags, since the assumed and actual conditions at the slot are so different.

When the boundary layer is laminar to the slot and the increase in momentum thickness across the slot is about $1 \cdot 25$, the agreement between the experimental and theoretical profile-drag coefficients is good. When the flow is turbulent, and the theoretical increase in momentum thickness is $4 \cdot 5$ for the Griffith aerofoil, the drag coefficient is overestimated by 50 per cent. A calculation has shown that an inconsistent assumption of momentum thickness remaining constant across the discontinuity results in an underestimation of profile drag (for the turbulent boundary layers) by 50 per cent.

It is clear that the effects of pressure gradient through the boundary layer are too large to be ignored, yet their inclusion at this stage is impossible. More work is required on these effects near the slot. A simple procedure might be to use an average curvature of the streamlines to obtain an average pressure in the boundary layer. From these pressures fictitious values of U_1 and U_2 might be obtained from Bernoulli's equation to be used in the analysis of the present paper, but obviously this cannot be considered in this report.

The present method is applicable to aerofoils or passages in which no discontinuity occurs at the slot. In this case the Taylor criterion is not used, and the troublesome curvature effects disappear.

9. *Conclusions.*—The present paper should give a good insight into the behaviour of slot-suction aerofoils, especially of the Griffith type, and should serve as a basis for computing the performance of such aerofoils. Until more information is available on the nature of the flow in the vicinity of the slot, the results given by calculations based on the methods of this paper must be regarded as approximations only.

Detailed theoretical and experimental investigations in the neighbourhood of the slot are needed to allow for pressure rise through boundary layer and sink effect. More information is required on the development of turbulent boundary layers under pressure gradients in order to substantiate the boundary-layer calculations. The wide choice of relations between $\tau_0/\rho U^2$ and R_θ, and the scatter of experimental points for the turbulent flow over a flat plate, suggests the need for more accurate experimental data.

The two thick suction aerofoils whose power requirements have been considered here have very low ideal effective-drag coefficients at flight Reynolds numbers. It is for further experiments to decide what addition slot entry and duct losses will make to the pump drag. It is the authors' opinion that this can be kept low by the use of a sufficiently wide slot and ducting of large cross-sectional area. Thus the velocity into the slot and in the ducting will be low, and hence the loss of head, which is proportional to the square of the velocity, will also be small. It is assumed that efficient ducting exists between the slot and the pump.

The twin-slot aerofoil gives the lowest drag, but requires greater suction quantity than the single-slot aerofoil. The ideal effective drag of the twin-slot aerofoil is slightly greater than that of a 20 per cent thick low-drag section of normal design when transition is forward. But when transition is near the slot very much smaller drag coefficients may be obtained on the suction aerofoils. The low values achieved arise from the reduction of form drag and from the large extents of laminar flow. Further, gas-turbines have compressors that are highly efficient as pumps, and which may exceed the efficiency of the propulsive system. This is an additional factor in favour of the application of boundary-layer suction to aerofoils.

REFERENCES

No.	*Author*	*Title, etc.*
1	E. J. Richards, W. S. Walker and J. R. Greening	Tests of a Griffith Aerofoil in the 13 ft × 9 ft Wind Tunnel. R. & M. 2148. March, 1944.
2	N. Gregory	Note on Sir Geoffrey Taylor's Criterion for the Rate of Boundary Layer Suction at a Velocity Discontinuity. R. & M. 2496. May, 1947.
3	E. J. Richards, W. S. Walker and C. R. Taylor	Wind-tunnel Tests on a 30 per cent Suction Wing. R. & M. 2149. July, 1945.
4	N. Gregory and W. S. Walker ..	Further Wind Tunnel Tests on a 30 per cent Symmetrical Suction Aerofoil with a Movable Flap. R. & M. 2287. July, 1946.
5	V. M. Falkner	Simplified Calculation of the Laminar Boundary Layer. R. & M. 1895. January, 1942.
6	N. Tetervin	A Method for the Rapid Estimation of Turbulent Boundary Layer Thicknesses for Calculating Profile Drag. N.A.C.A. A.C.R. No. L4G14. A.R.C. 8498. July, 1944. (Unpublished.)
7	M. Holt	Calculations of Wing Profile Drag. *Aircraft Engineering*. Vol. XV. No. 176, pp. 278–280. October, 1943.
8	B. Thwaites	On the Use of the Momentum Equation in Laminar Boundary Layer Flow. Part III. A General and Simplified Method of Solution for Solid Boundaries. A.R.C. 11,157. 1947. (Unpublished.)
9	S. Goldstein (ed.)	*Modern Developments in Fluid Dynamics*. Vol. I. Chapter IV. Section 60. Oxford University Press.
10	H. B. Squire and A. D. Young ..	The Calculation of the Profile Drag of Aerofoils. R. & M. 1838. November, 1938.
11	M. B. Glauert	The Design of Suction Aerofoils with a Very Large C_L-Range. R. & M. 2111. November, 1947.
12	M. J. Lighthill	A New Method of Two-dimensional Aerodynamic Design. R. & M. 2112. April, 1945.
13	S. Goldstein	A Theory of Aerofoils of Small Thickness. Part I. A.R.C. 6225. 1942. (To be published.)
14	R. C. Lock	Note on Profile Drag Calculations for Low Drag Wings with Cusped Trailing Edges. R. & M. 2419. April, 1946.
15	J. Ackeret	Probleme des Flugzeugantriebs in Gegenwart und Zukunft. *Schweiz. Bauzeitung*. Bd. 112, No. 1. 1938.

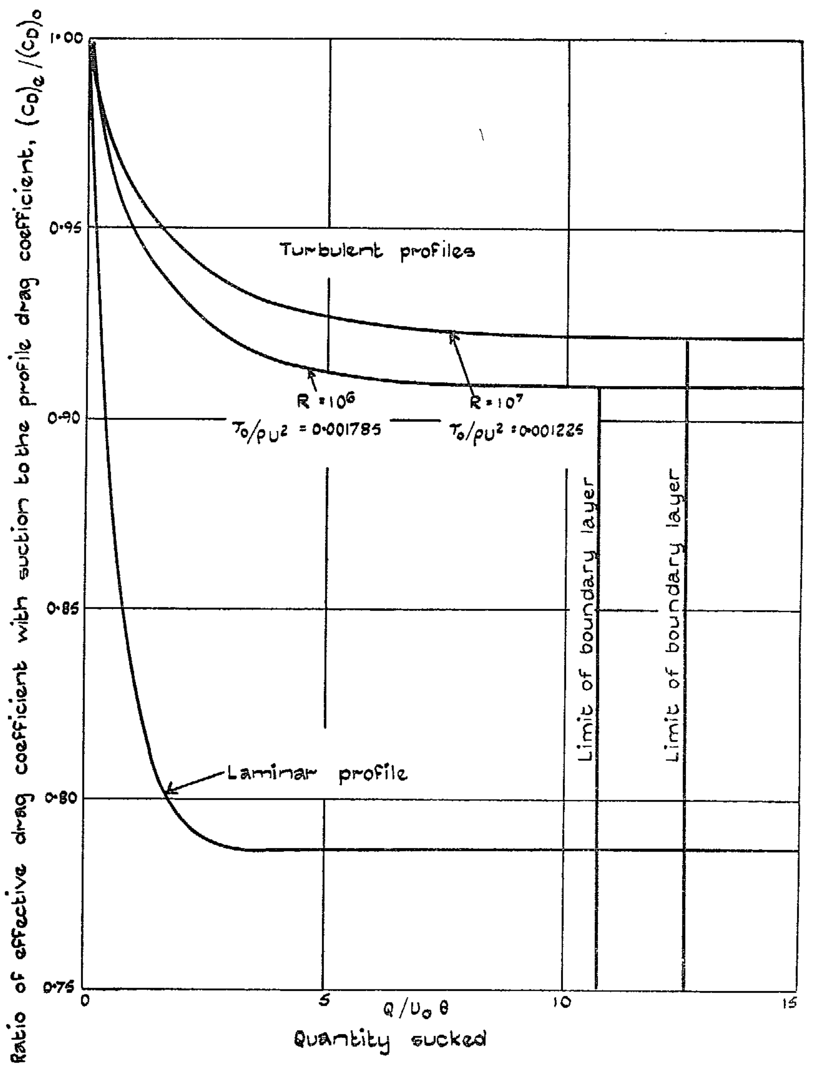

FIG. 1. Variation of effective-drag coefficient of flat plate with amount of boundary layer sucked.

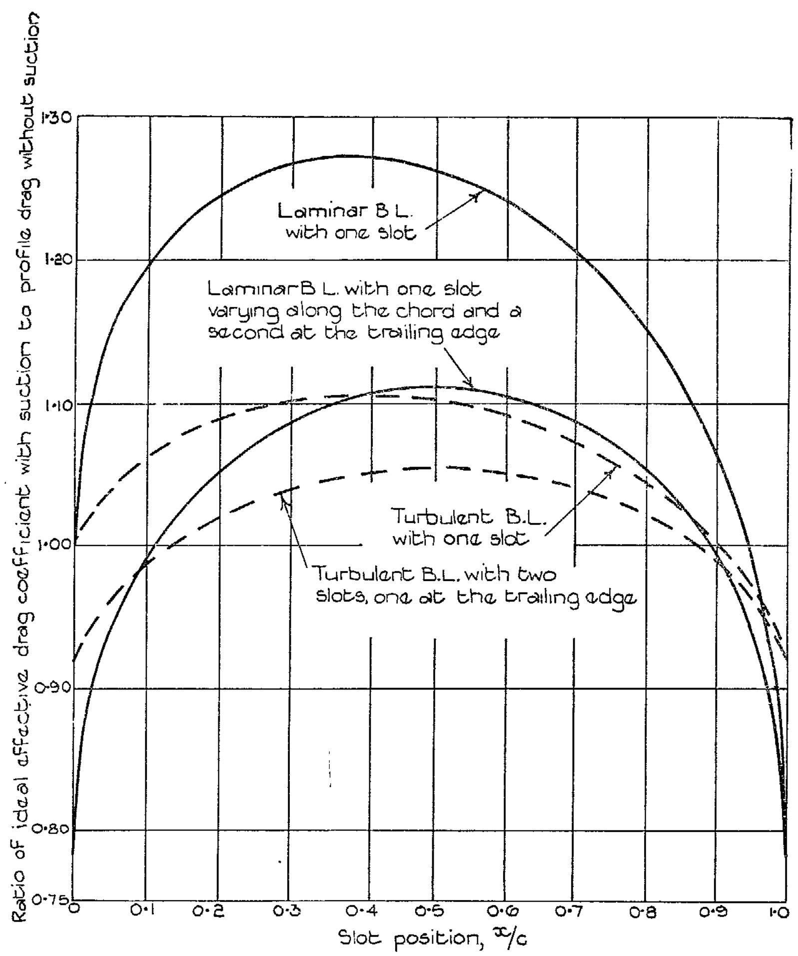

FIG. 2. Variation of the effective-drag coefficient of a flat plate with boundary-layer suction-slot position.

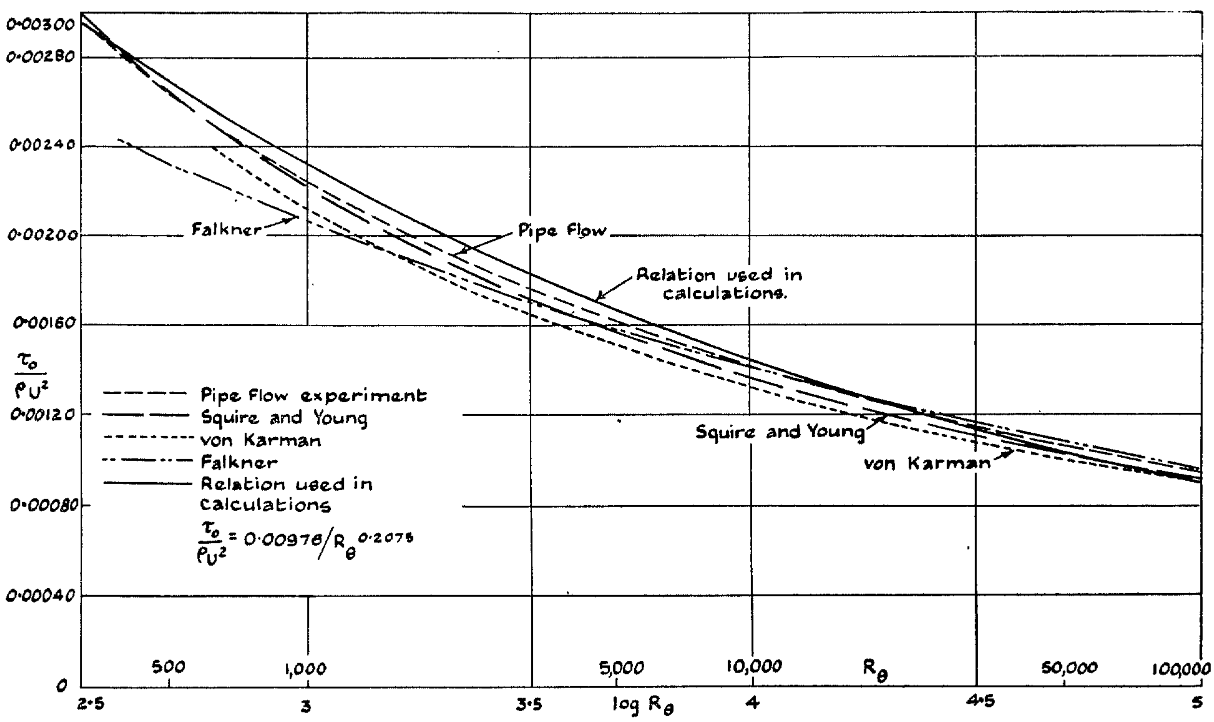

FIG. 3. Relation between τ_0 and R_θ, $\tau_0/\rho U^2 = 0{\cdot}00976/R_\theta^{0{\cdot}2075}$, used in momentum thickness calculations, giving good agreement with existing skin-friction curves over whole range of R_θ.

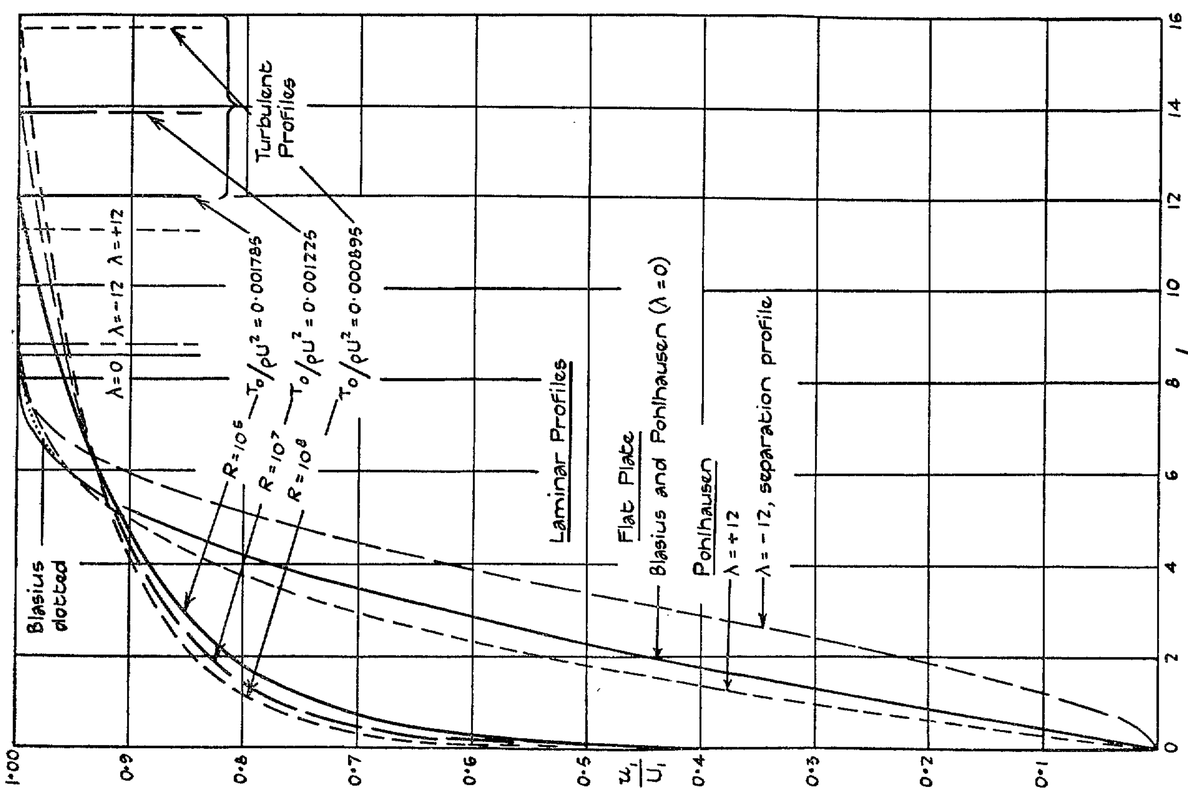

FIG. 4. Velocity profiles just ahead of suction slot.

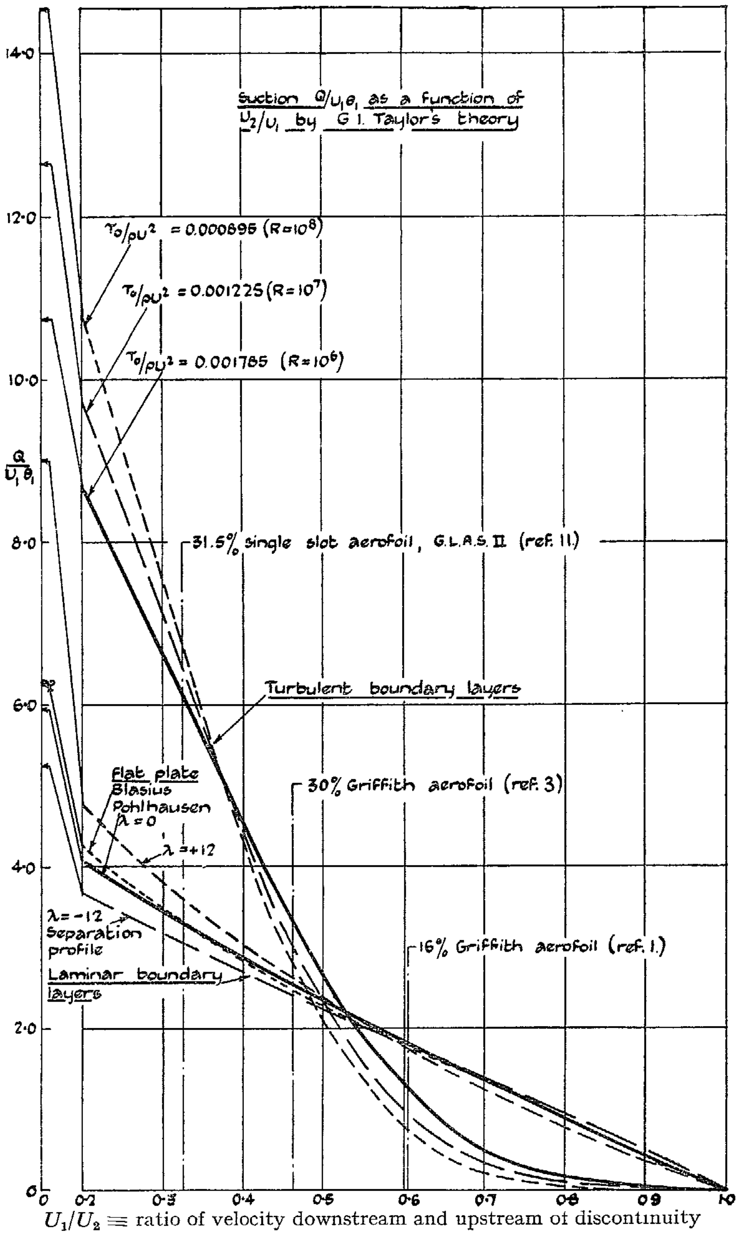

FIG. 5. Suction $Q/U_1\theta_1$ as a function of U_2/U_1 by G. I. Taylor's theory.

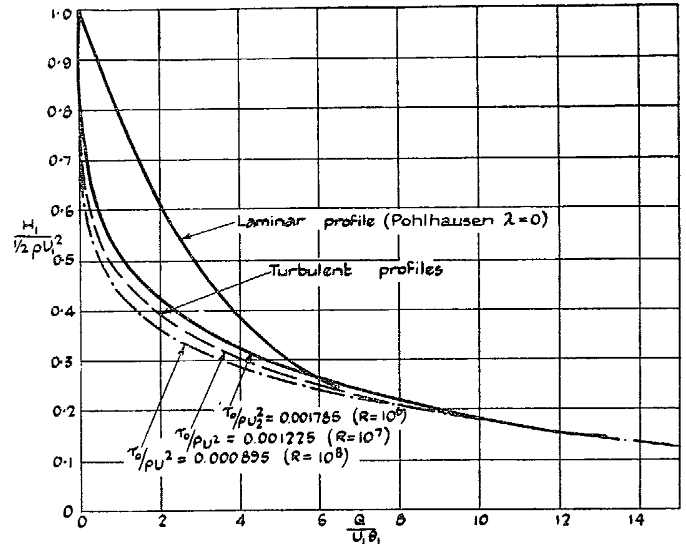

(a) Mean loss of head for quantity Q sucked as a function of $Q/U_1\theta_1$

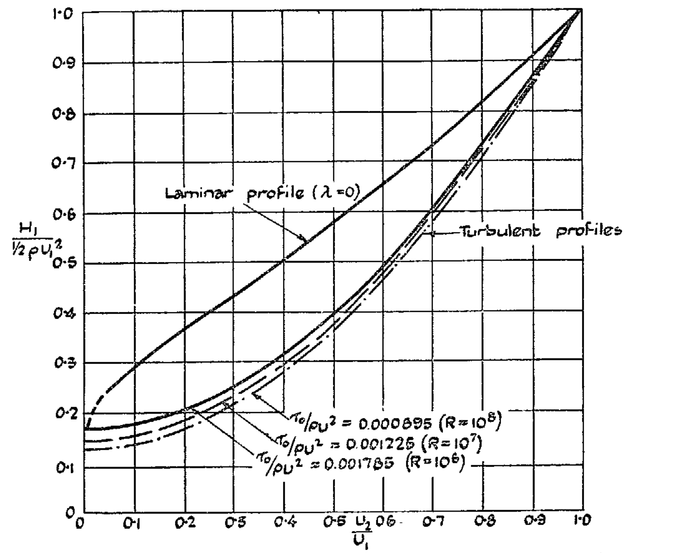

(b) Mean loss of head as a function of discontinuity (Q given by G.I. Taylor's theory)

FIG. 6.

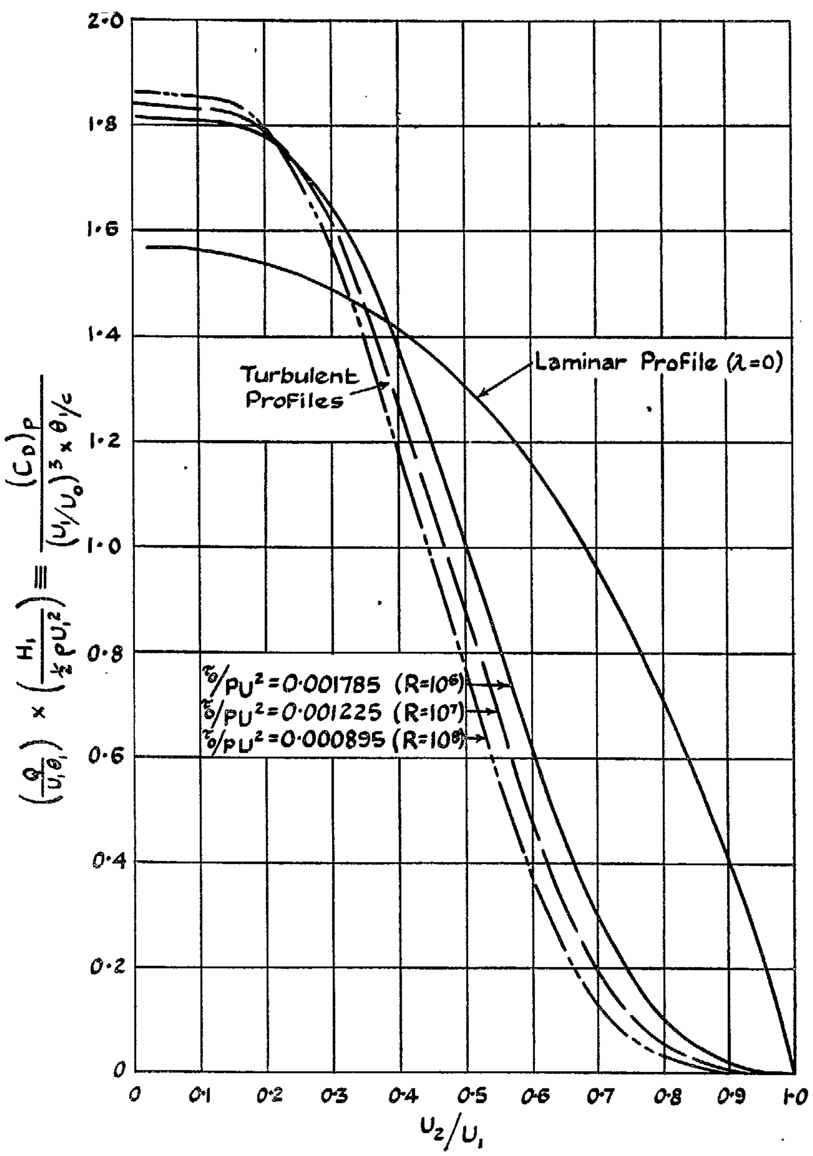

FIG. 7. Ideal pump-drag coefficient given as a function of discontinuity.

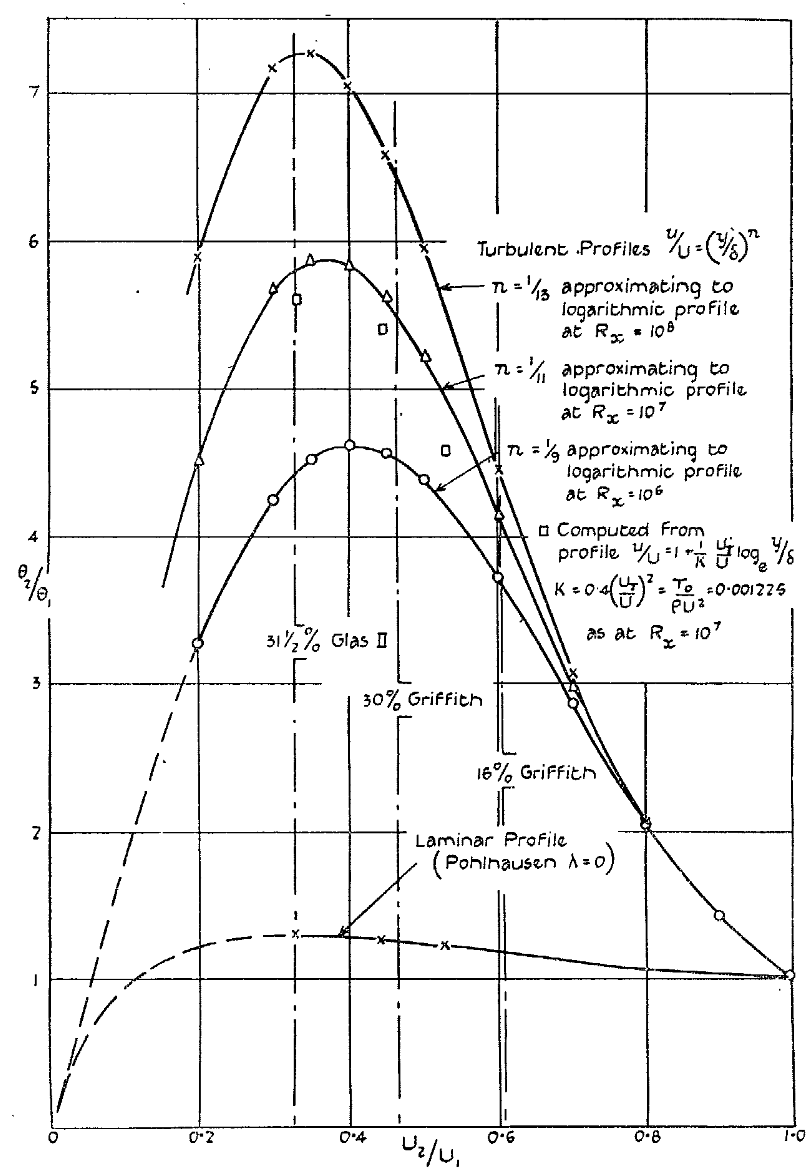

FIG. 8. Relation between ratio of momentum thicknesses across slot and the discontinuity. Suction according to Taylor's criterion.

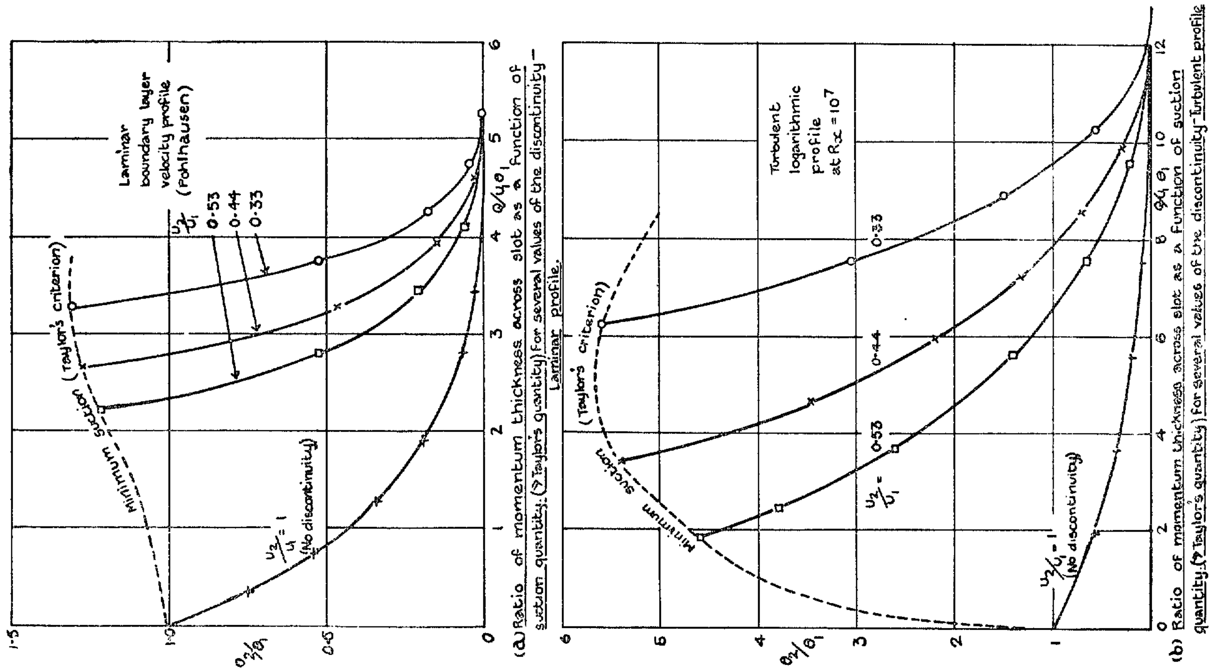

FIG. 9.

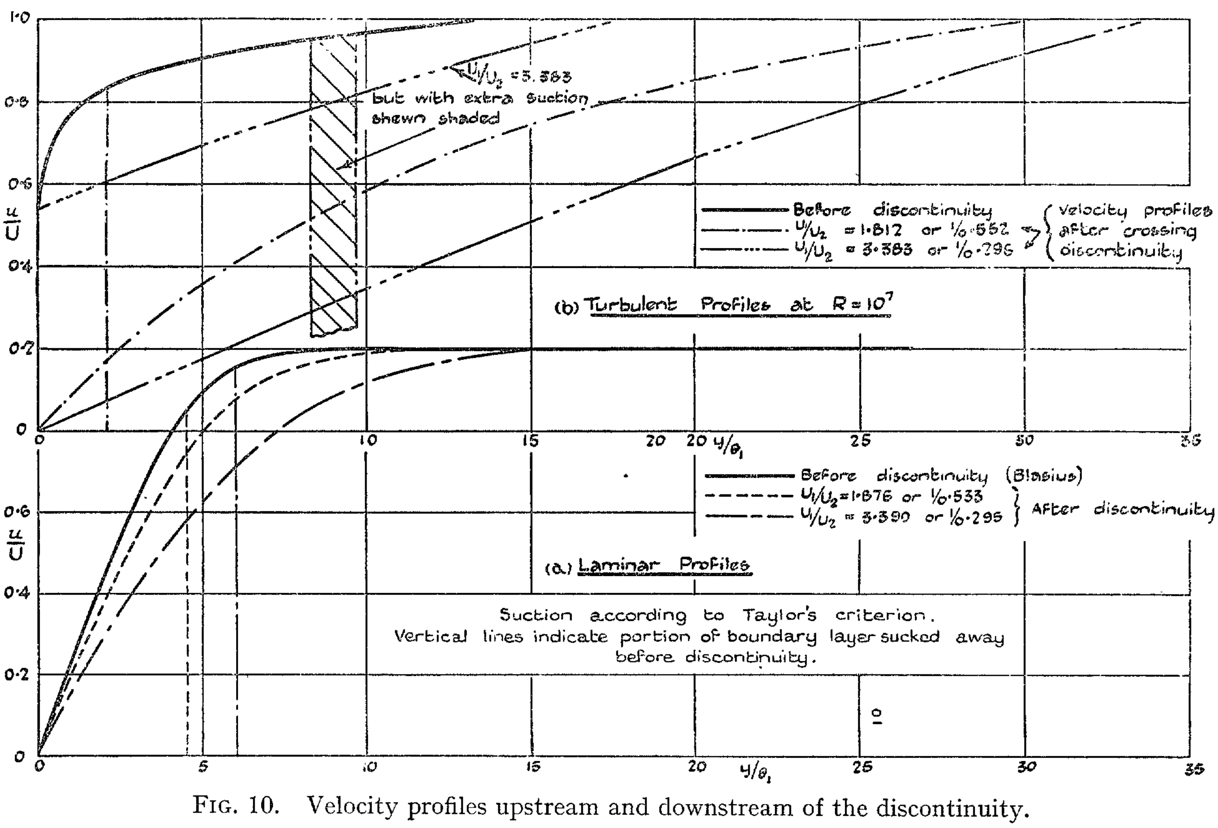

FIG. 10. Velocity profiles upstream and downstream of the discontinuity.

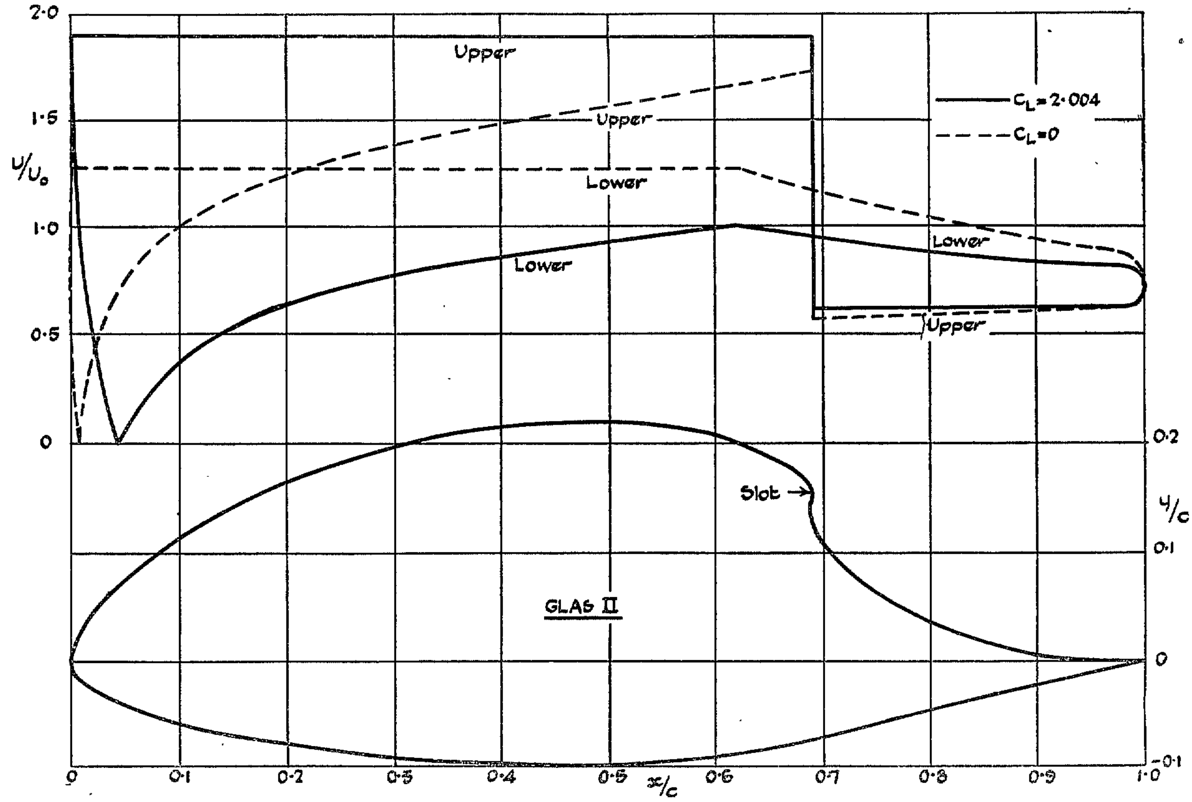

FIG. 11. GLAS II aerofoil and velocity distribution.

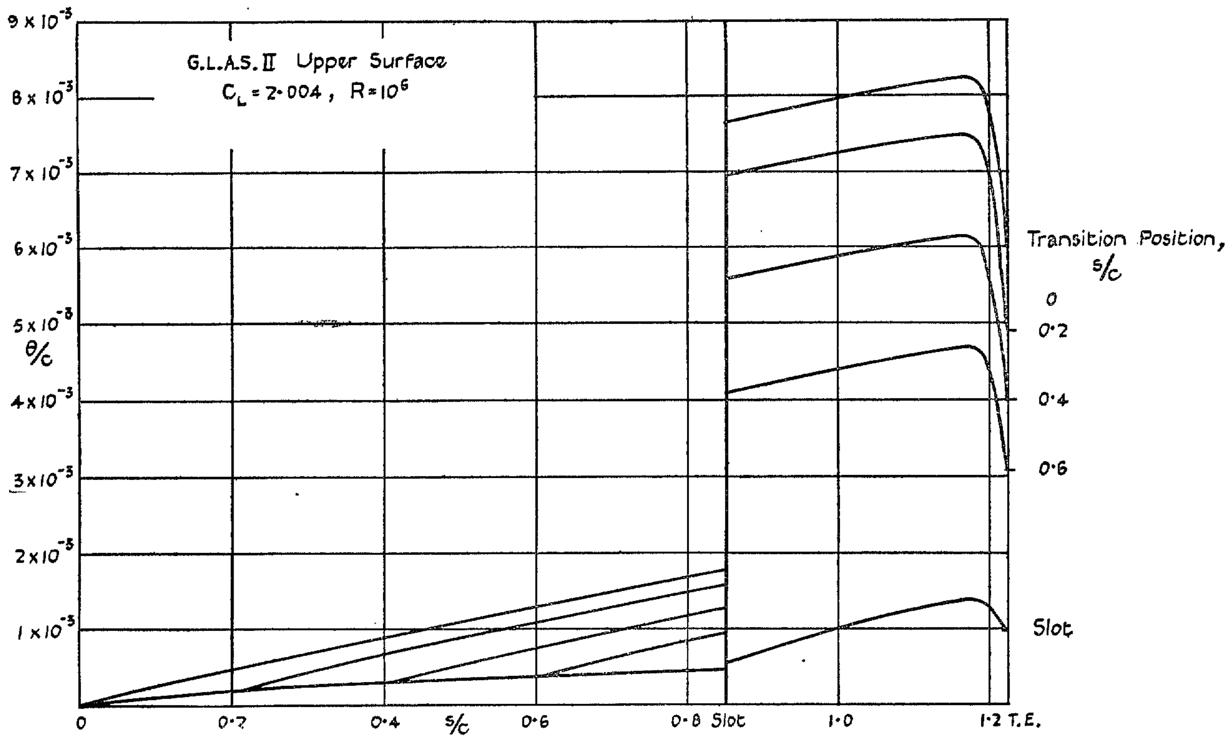

FIG. 12. Variation of momentum thickness along surfaces of GLAS II aerofoil with different transition positions.

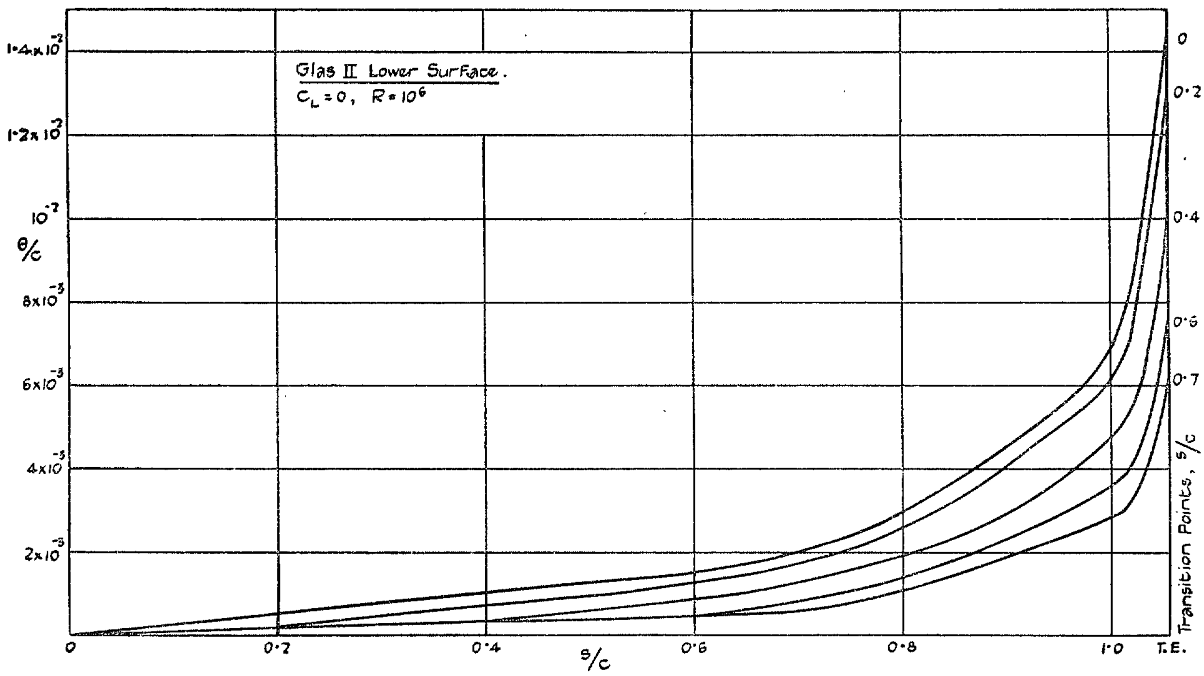

FIG. 13. Variation of momentum thickness along surfaces of GLAS II aerofoil with different transition positions.

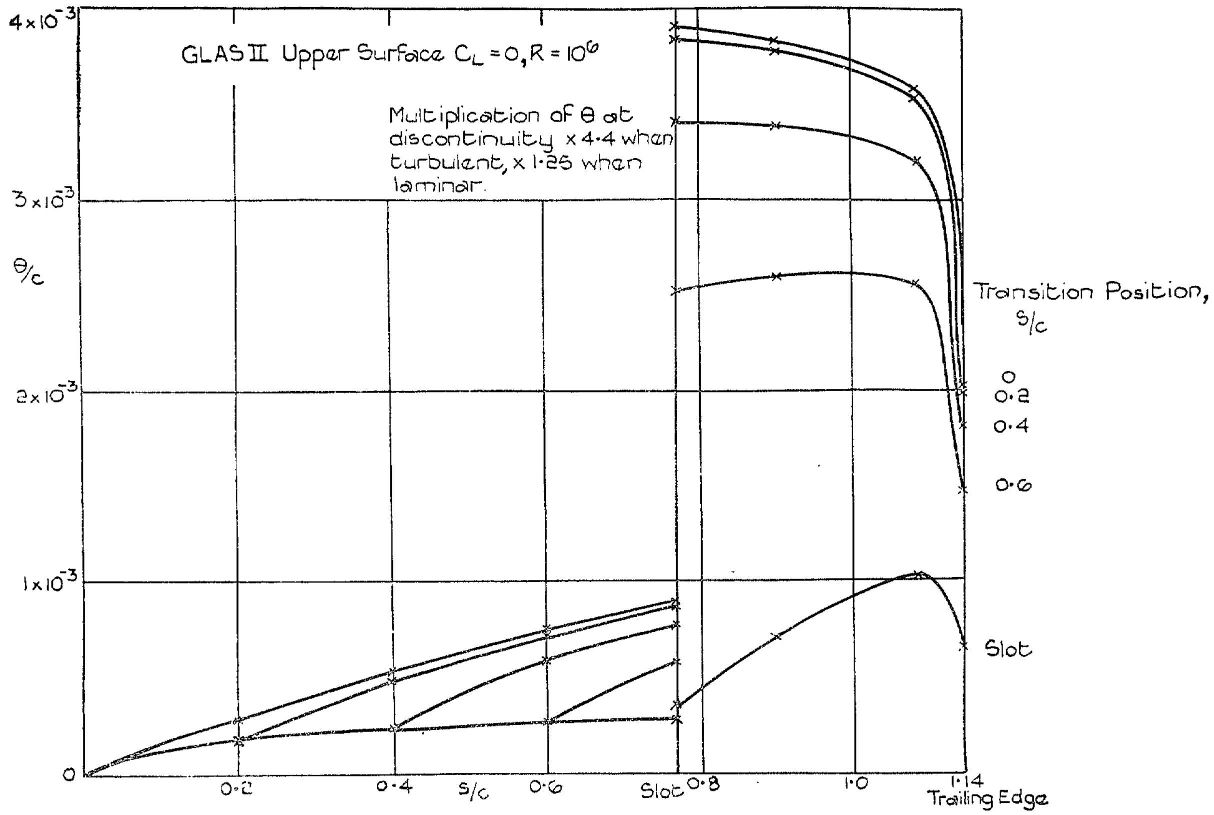

FIG. 14. Variation of momentum thickness along surfaces of GLAS II aerofoil with different transition positions.

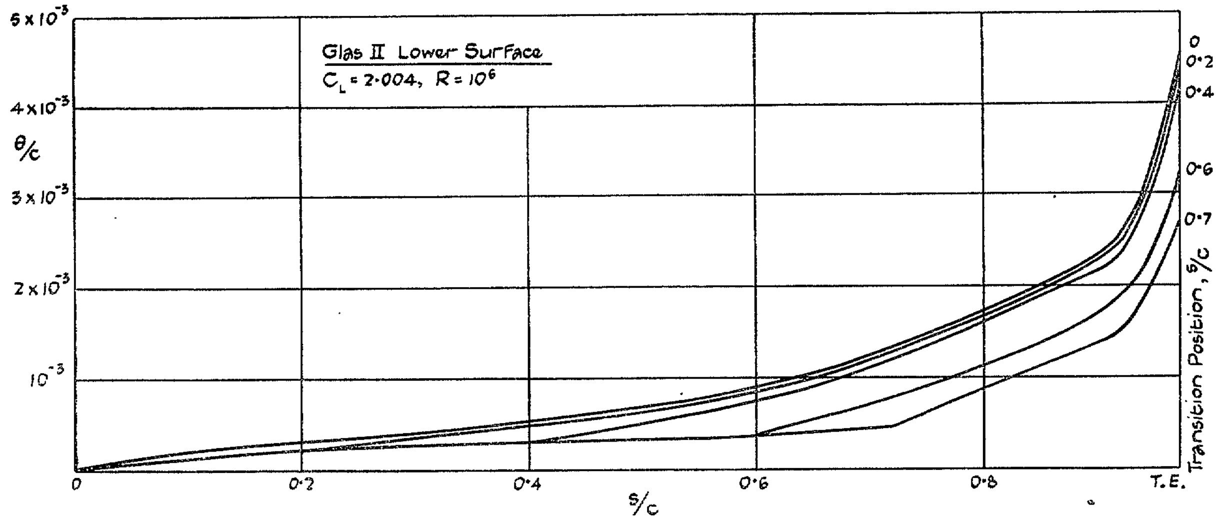

FIG. 15. Variation of momentum thickness along surfaces of GLAS II aerofoil with different transition positions.

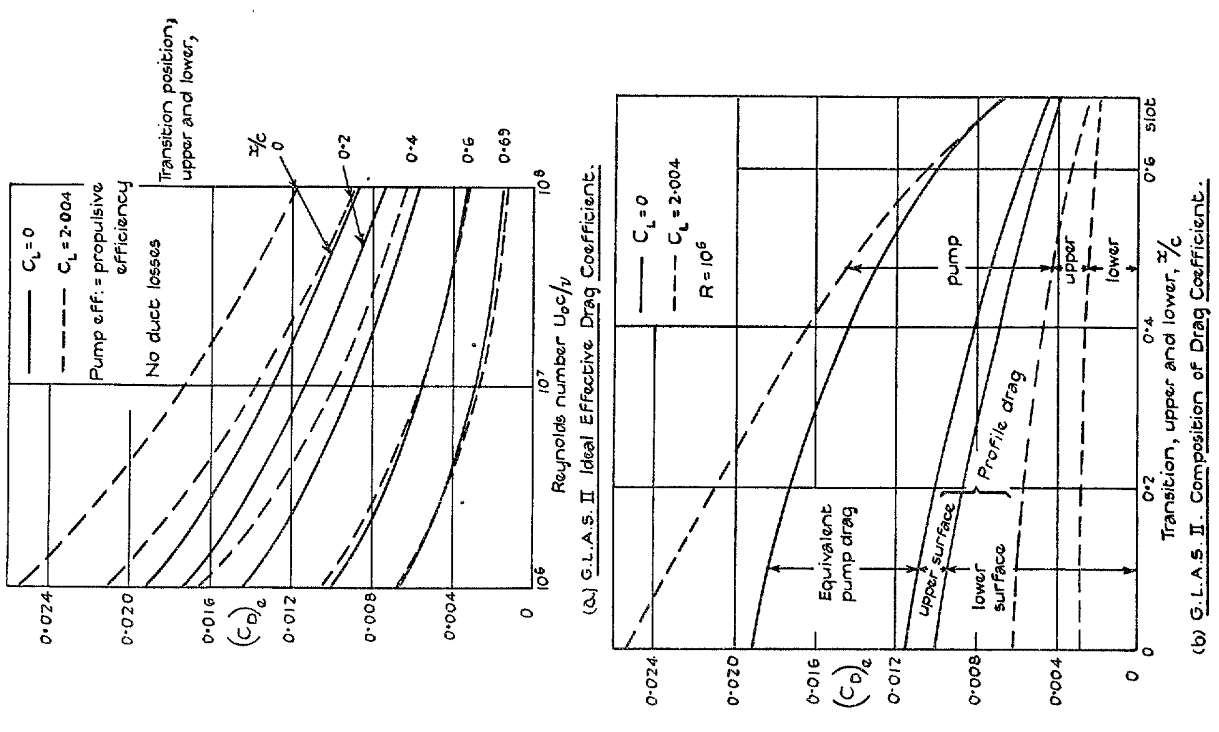

FIGS. 16a and b.

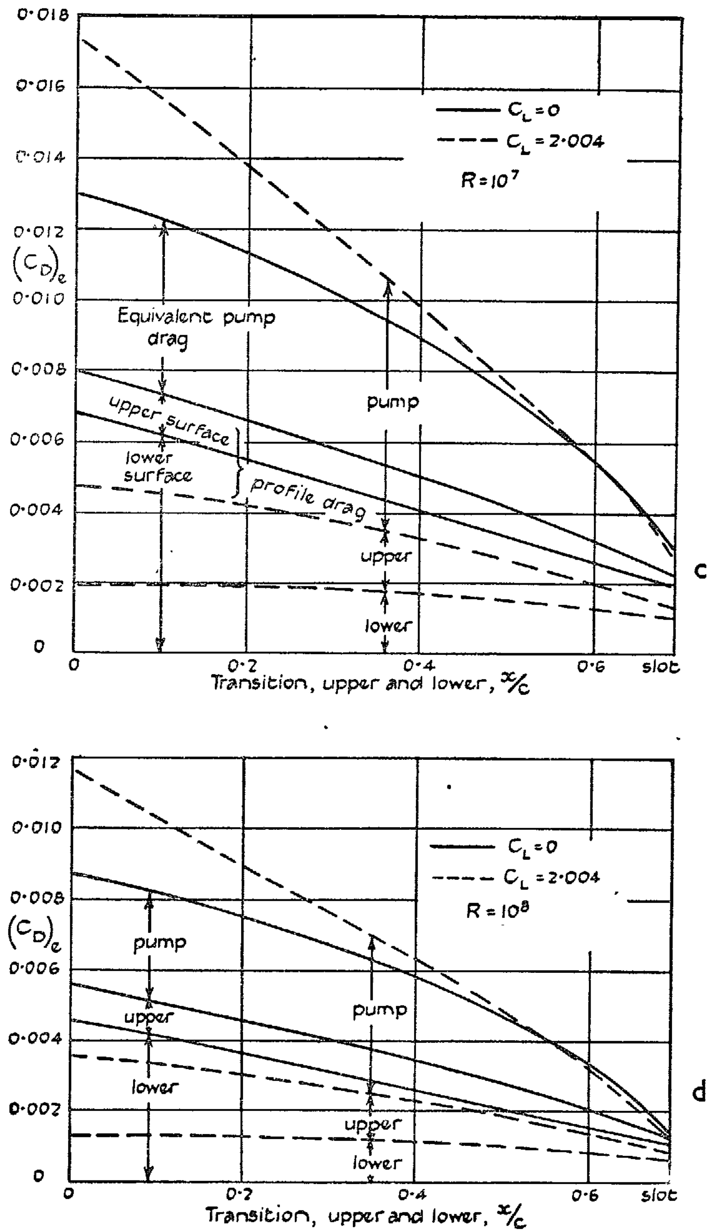

FIGS. 16 c and d. GLAS II. Composition of drag coefficient.

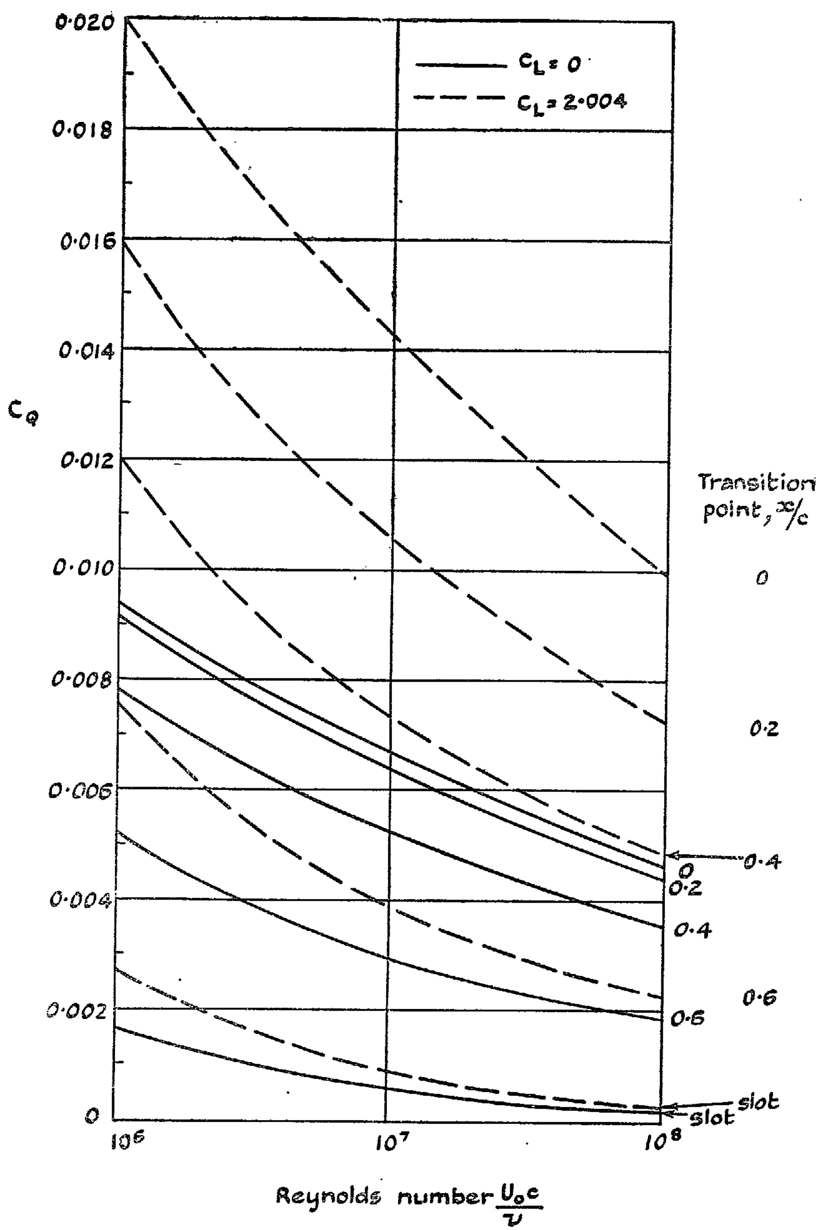

FIG. 17. GLAS II pump quantity coefficient $C_Q = Q/U_0c$ against Reynolds number for various transition positions x/c.

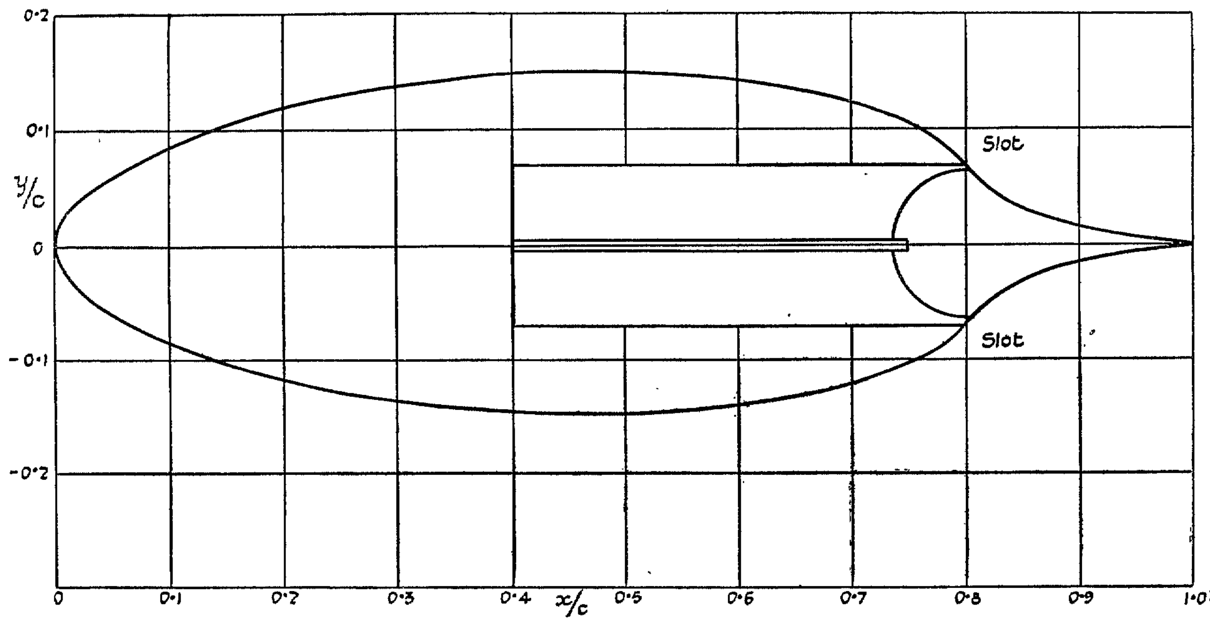

FIG. 18a. 30 per cent suction wing with cusped tail. $x_1 = 0 \cdot 8$, $a = 0 \cdot 260242$, $b = 0 \cdot 426414$, $d = 0 \cdot 288803$, $(b - c) = 0 \cdot 756361$.

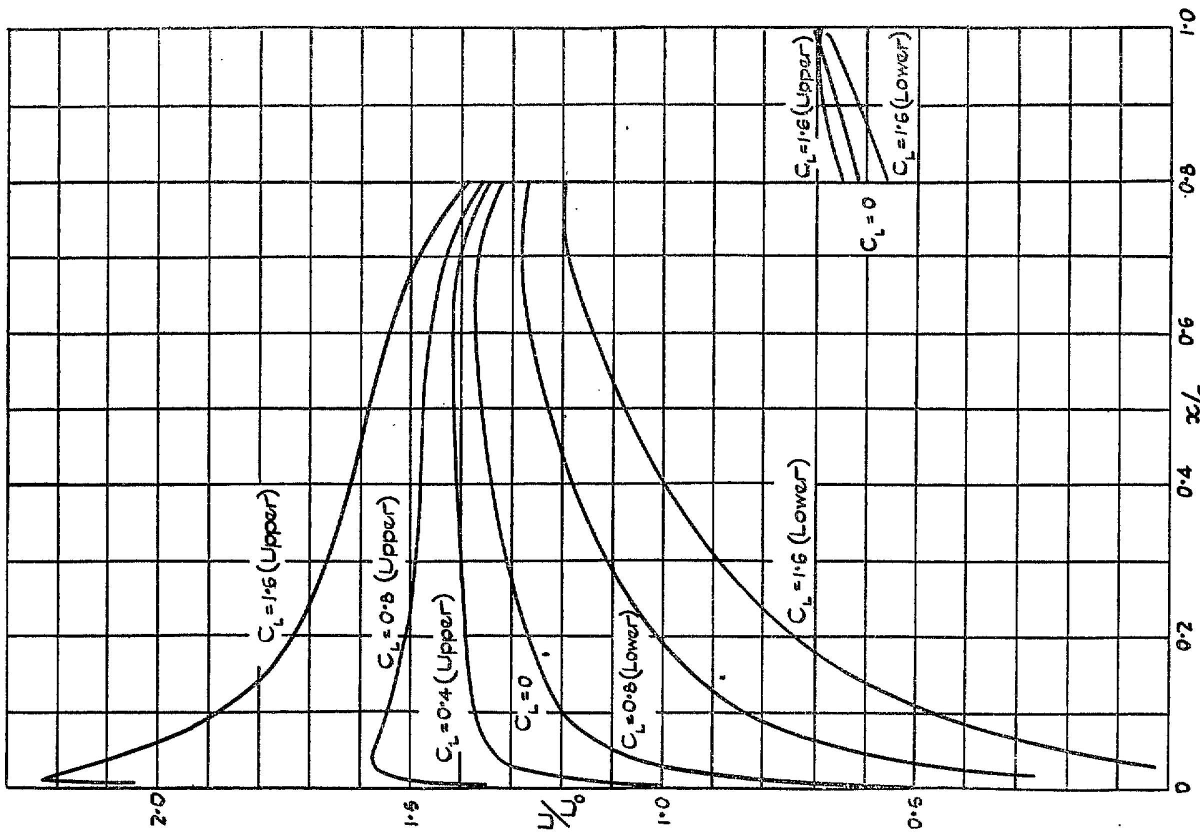

FIG. 18b. Theoretical velocity distribution over 30 per cent suction wing. $a_0 = 7 \cdot 9$. Approximation III of Ref. 13.

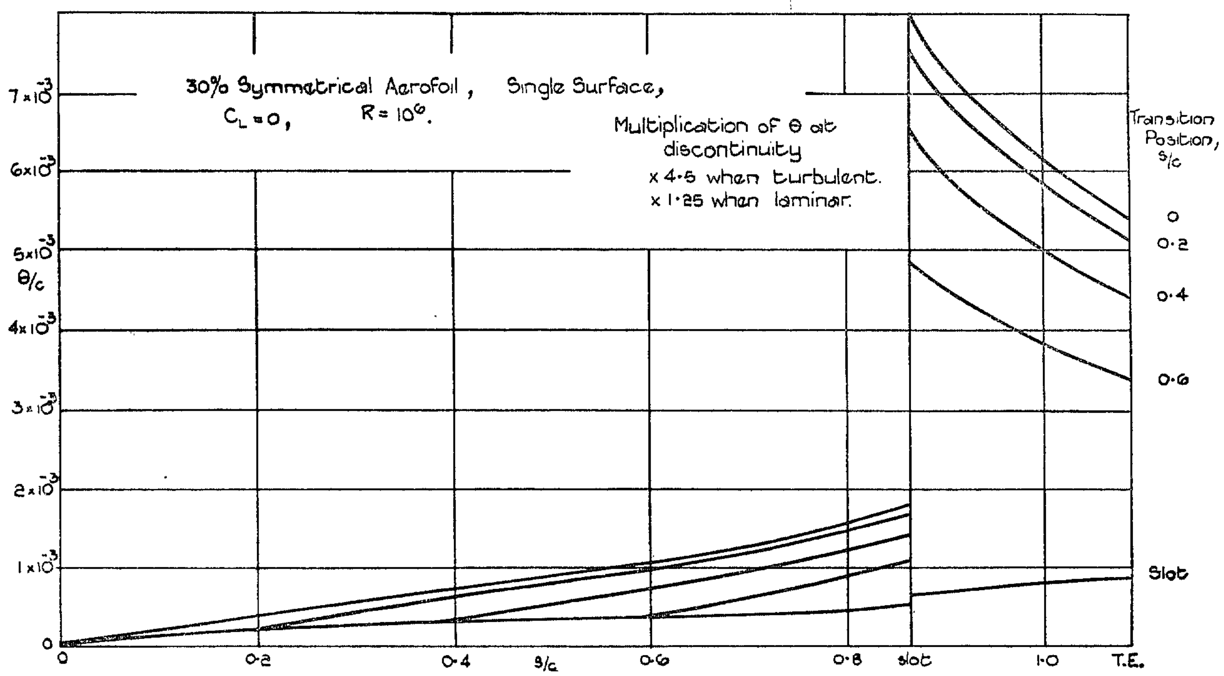

FIG. 19. Variation of momentum thickness along surface of 30 per cent symmetrical aerofoil with different transition positions.

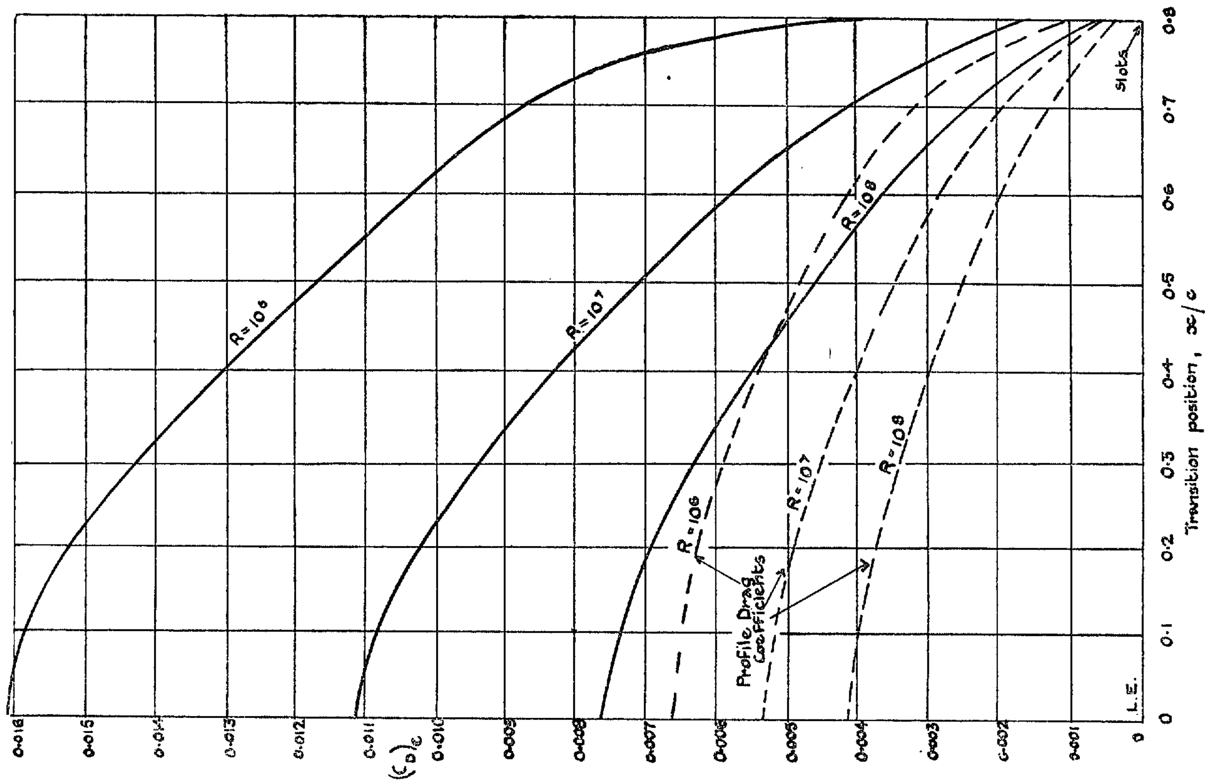

FIG. 20. Composition of ideal effective-drag coefficient, 30 per cent symmetrical aerofoil. $C_L = 0$. pump efficiency = propulsive efficiency. No duct losses.

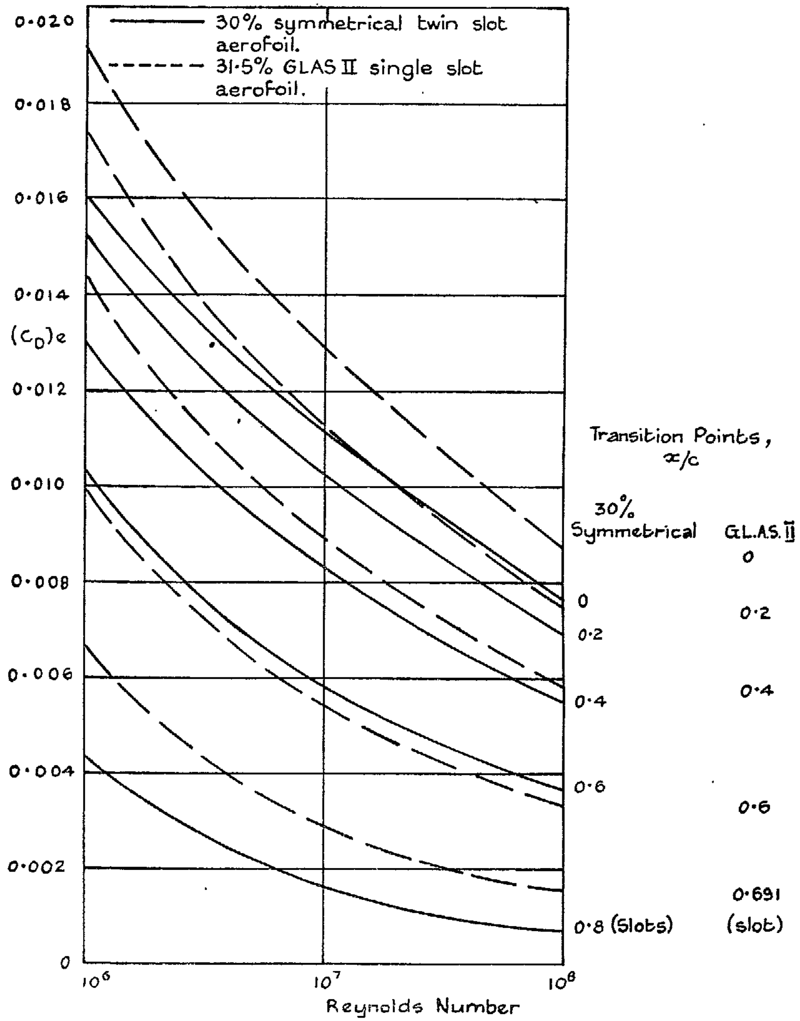

FIG. 21. Ideal effective-drag coefficient against Reynolds number for various transition positions. $C_L = 0$.

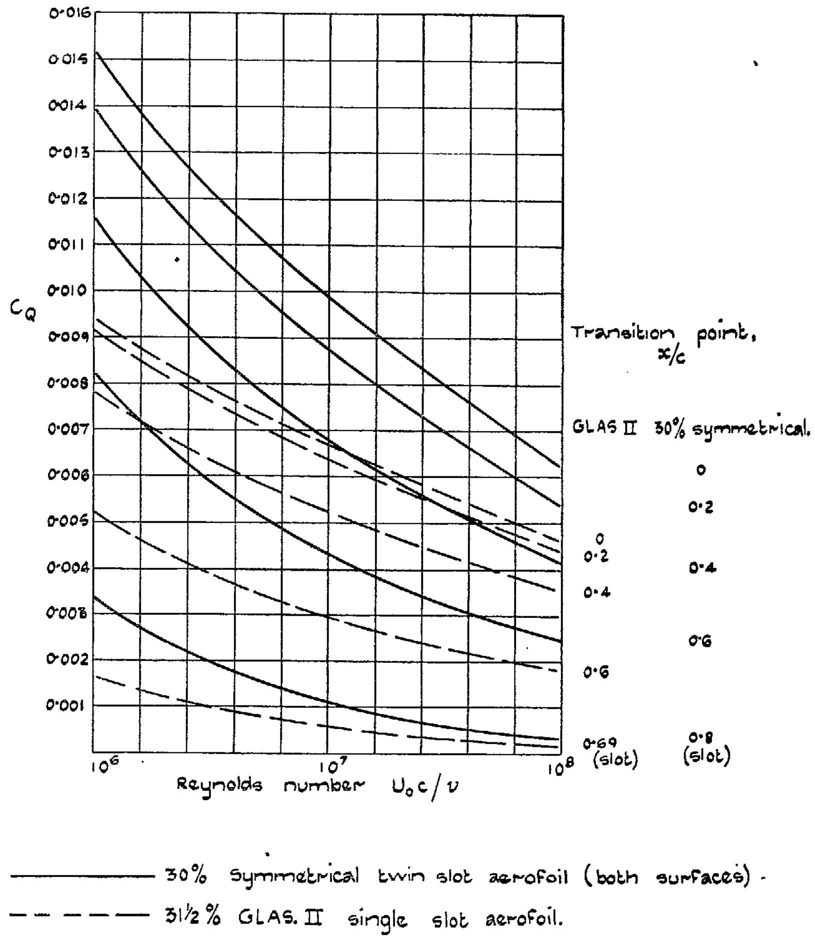

FIG. 22. Overall suction quantity coefficient C_Q against Reynolds number for various transition positions. $C_L = 0$.

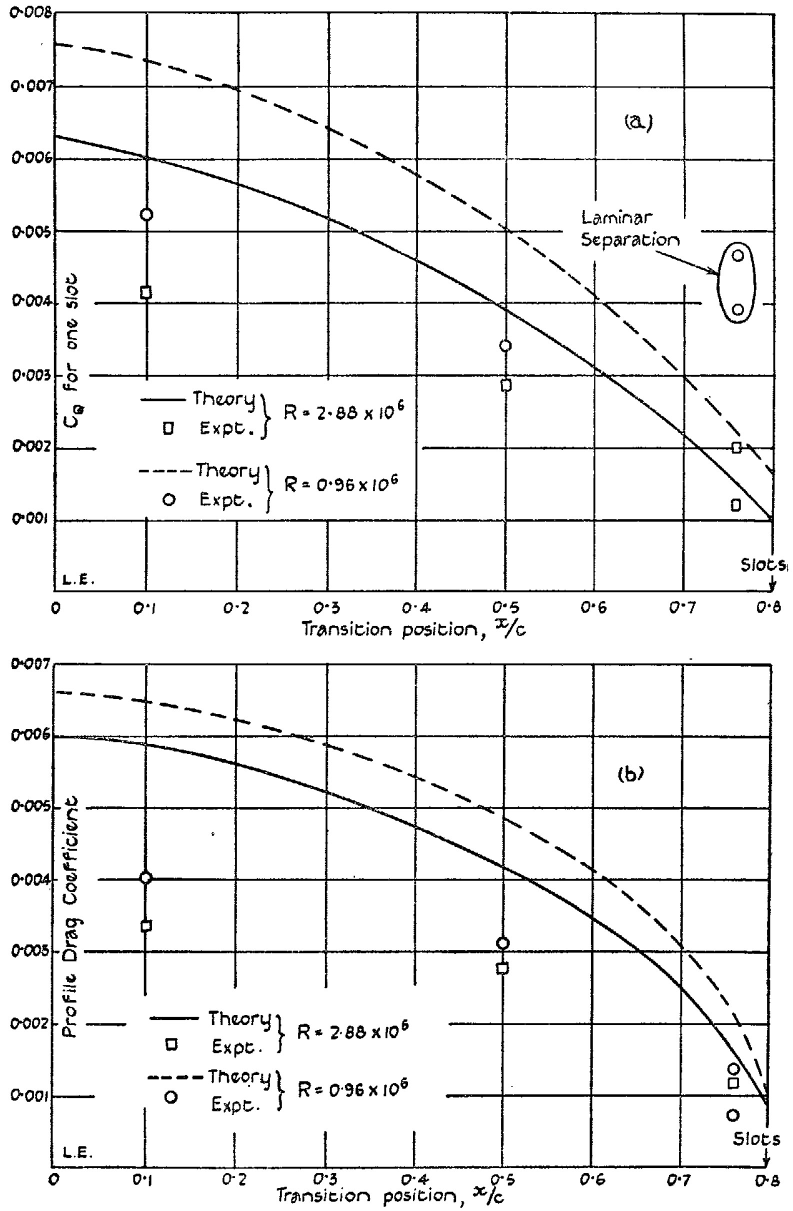

FIG. 23. 30 per cent symmetrical aerofoil. Comparison of theory and experiment.

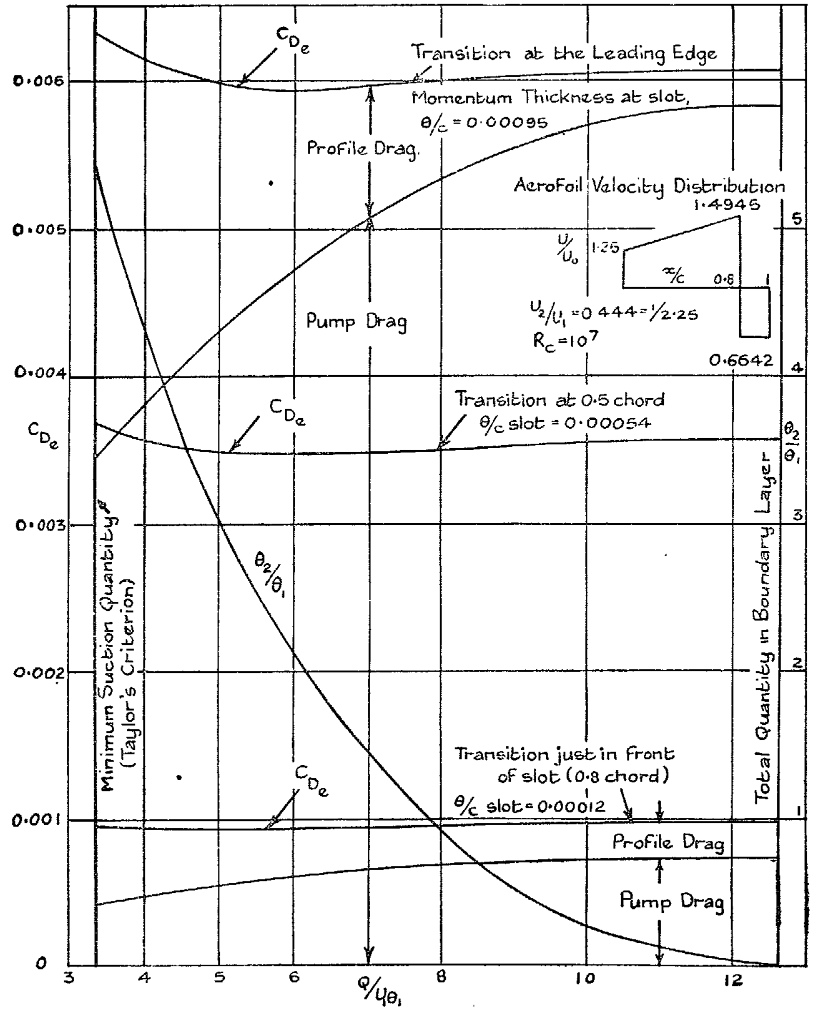

FIG. 24. Variation of ideal effective-drag coefficient with suction quantity for a turbulent boundary layer at the slot position.

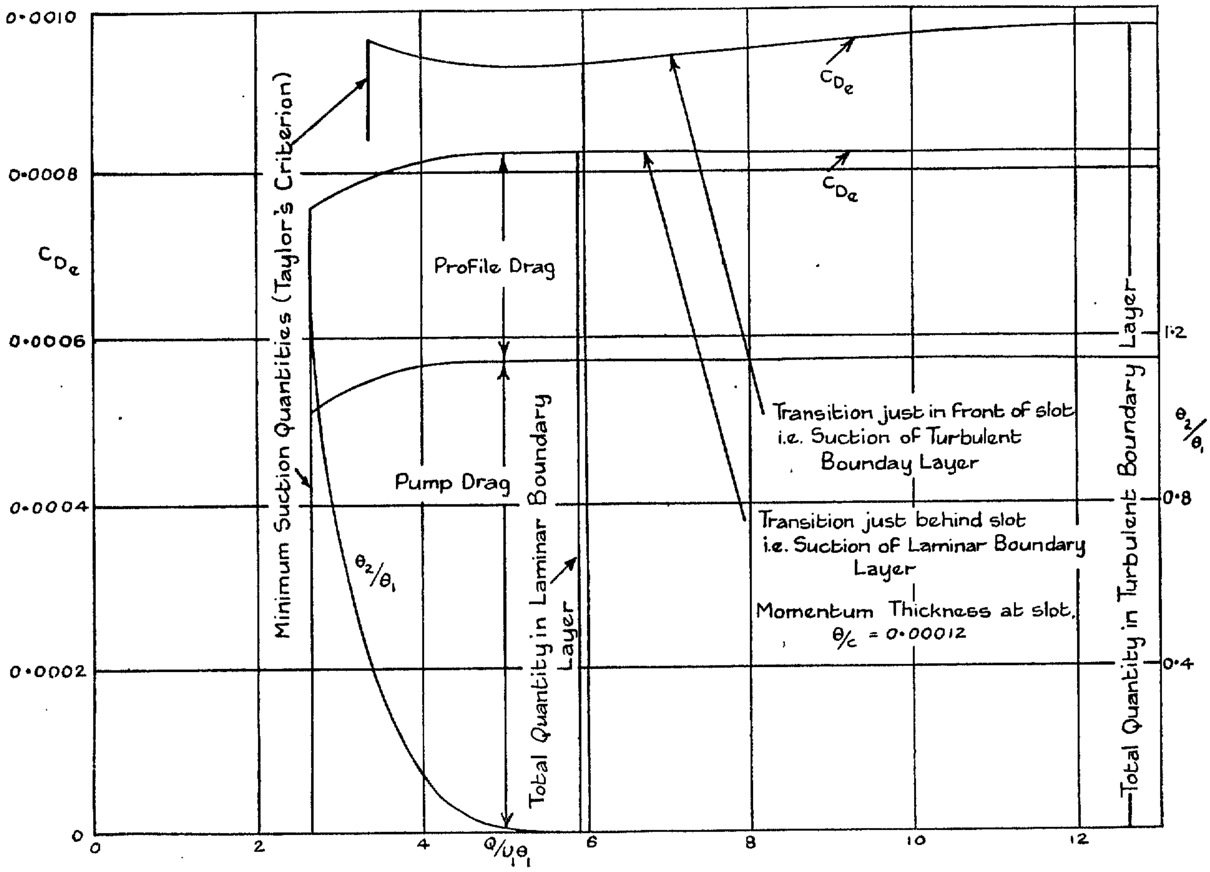

FIG. 25. Variation of ideal effective-drag coefficient with suction quantity for a laminar boundary layer to slot position.

Wt. .4/655 K.9 1/53 G.G. 34-262

PRINTED IN GREAT BRITAIN

Publications of the Aeronautical Research Council

ANNUAL TECHNICAL REPORTS OF THE AERONAUTICAL RESEARCH COUNCIL (BOUND VOLUMES)

1936 Vol. I Aerodynamics General, Performance, Airscrews, Flutter and Spinning. 40s. (40s. 9d.)
Vol. II Stability and Control, Structures, Seaplanes, Engines, etc. 50s. (50s. 10d.)

1937 Vol. I. Aerodynamics General, Performance, Airscrews, Flutter and Spinning. 40s. (40s 10d.)
Vol. II. Stability and Control, Structures, Seaplanes, Engines, etc. 60s. (61s.)

1938 Vol. I Aerodynamics General, Performance, Airscrews. 50s. (51s.)
Vol. II. Stability and Control, Flutter, Structures, Seaplanes, Wind Tunnels, Materials 30s. (30s 9d.)

1939 Vol. I. Aerodynamics General, Performance, Airscrews, Engines. 50s. (50s. 11d.)
Vol. II. Stability and Control, Flutter and Vibration, Instruments, Structures, Seaplanes, etc. 63s. (64s. 2d)

1940 Aero and Hydrodynamics, Aerofoils, Airscrews, Engines, Flutter, Icing, Stability and Control, Structures, and a miscellaneous section. 50s. (51s.)

1941 Aero and Hydrodynamics, Aerofoils, Airscrews, Engines, Flutter, Stability and Control, Structures 63s. (64s. 2d.)

1942 Vol I. Aero and Hydrodynamics, Aerofoils, Airscrews, Engines. 75s. (76s. 3d)
Vol. II. Noise, Parachutes, Stability and Control, Structures, Vibration, Wind Tunnels. 47s. 6d. (48s. 5d.)

1943 Vol. I. (In the press.)
Vol. II. (In the press.)

ANNUAL REPORTS OF THE AERONAUTICAL RESEARCH COUNCIL—

1933–34	1s. 6d. (1s. 8d.)	1937	2s. (2s. 2d)
1934–35	1s 6d. (1s. 8d.)	1938	1s. 6d (1s. 8d.)
April 1, 1935 to Dec. 31, 1936	4s. (4s. 4d.)	1939–48	3s. (3s 2d.)

INDEX TO ALL REPORTS AND MEMORANDA PUBLISHED IN THE ANNUAL TECHNICAL REPORTS, AND SEPARATELY—

April, 1950 .. .. R. & M. No. 2600. 2s. 6d. (2s. 7½d.)

AUTHOR INDEX TO ALL REPORTS AND MEMORANDA OF THE AERONAUTICAL RESEARCH COUNCIL—

1909–1949 . .. . R. & M. No. 2570. 15s. (15s. 3d.)

INDEXES TO THE TECHNICAL REPORTS OF THE AERONAUTICAL RESEARCH COUNCIL—

December 1, 1936 — June 30, 1939	R. & M No. 1850.	1s. 3d. (1s. 4½d)
July 1, 1939 — June 30, 1945	R. & M. No. 1950	1s. (1s. 1½d)
July 1, 1945 — June 30, 1946	R & M. No. 2050	1s. (1s. 1½d.)
July 1, 1946 — December 31, 1946	R. & M. No. 2150.	1s. 3d (1s. 4½d.)
January 1, 1947 — June 30, 1947	R. & M. No. 2250.	1s. 3d (1s. 4½d.)
July, 1951	R. & M. No. 2350.	1s. 9d. (1s 10½d)

Prices in brackets include postage.

Obtainable from

HER MAJESTY'S STATIONERY OFFICE

York House, Kingsway, London, W.C.2; 423 Oxford Street, London, W.1 (Post Orders: P.O. Box 569, London, S.E.1); 13a Castle Street, Edinburgh 2; 39 King Street, Manchester 2; 2 Edmund Street, Birmingham 3; 1 St. Andrew's Crescent, Cardiff; Tower Lane, Bristol 1; 80 Chichester Street, Belfast,
OR THROUGH ANY BOOKSELLER